2021-11

FINITE ELEMENT STUDY ON FLEXURAL PERFORMANCE OF CARBON FIBER REINFORCED POLYMER GRID REINFORCED TWO WAY SLAB SYSTEM

MASTEWAL, TSEGAYE GETANEH

BAHIR DAR UNIVERSITY

BAHIR DAR INSTITUTE OF TECHNOLOGY

SCHOOL OF RESEARCH AND POSTGRADUATE STUDIES

FACULTY OF CIVIL AND WATER RESOURCES ENGINEERING

FINITE ELEMENT STUDY ON FLEXURAL PERFORMANCE OF CARBON FIBER REINFORCED POLYMER GRID REINFORCED TWO WAY SLAB SYSTEM

BY

MASTEWAL TSEGAYE GETANEH

BAHIR DAR, ETHIOPIA

November, 2021

FINITE ELEMENT STUDY ON FLEXURAL PERFORMANCE OF CARBON FIBER REINFORCED POLYMER GRID REINFORCED TWO WAY SLAB SYSTEM

BY

MASTEWAL TSEGAYE GETANEH

A thesis submitted to the school of Research and Graduate Studies of Bahir Dar Institute of Technology, BDU in partial fulfillment of the requirements for the degree of

Master degree in structural engineering in the facility of civil and water resource engineering.

Advisor Name: Tesfaye Alemu (PhD)

Co-Advisor Name:

Bahir Dar, Ethiopia

November, 2021

DECLARATION

This is to certify that the thesis entitled "**Finite element study on flexural performance of carbon fiber reinforced polymer grid reinforced two way slab system**" submitted in partial fulfillment of the requirements for the degree of Master of Science in structural engineering under faculty of civil and water resources engineering, Bahir Dar Institute of Technology, is a record of original work carried out by me and has never been submitted to this or any other institution to get any other degree or certificates. The assistance and help I received during the course of this investigation have been duly acknowledged.

Mastewal Tsegaye	MTS	5-10-2021
Name of the candidate	signature	Date

BAHIR DAR UNIVERSITY

BAHIR DAR INSTITUTE OF TECHNOLOGY

SCHOOL OF RESEARCH AND GRADUATE STUDIES

FACULTY OF CIVIL AND WATER RESOURCE ENGINEERING

Approval of thesis for defense result

I hereby confirm that the changes required by the examiners have been carried out and incorporated in the final thesis.

Name of Student: Mastewal Tsegaye Signature _____ Date 15-11-2021

As members of the board of examiners, we examined this thesis entitled "**Finite element study on flexural performance of carbon fiber reinforced polymer grid reinforced two way slab system**" by **Mastewal Tseagye**. We hereby certify that the thesis is accepted for fulfilling the requirements for the award of the degree of Masters of Science in "Structural engineering".

Board of Examiners

Name of Advisor	Signature	Date
Dr. Tesfaye Alemu		03/11/2021
Name of External examiner	Signature	Date
Dr.Kabtamu Getachew		02/11/2021
Name of Internal Examiner	Signature	Date
Seto Meless		12-11-2021
Name of Chairperson	Signature	Date
Muluget Assefa		15-11-2021
Name of Chair Holder	Signature	Date
Wasihun Moges		15/11/2021
Name of Faculty Dean	Signature	Date
Temesgen Enku Nigussie (PhD) Faculty Dean		NOV. 15, 2021

Dedicated to my grand father

ACKNOWLEDGEMENT

First and foremost, praises and thanks to GOD for his endless blessing, helping and for giving me the power, strength and wisdom to complete my thesis work successfully and in every achievement throughout my life.

Great thanks deserve to my former teacher and now advisor Dr. Tesfaye Alemu for his unlimited support and sharing his knowledge openly.

I also would like to thank my friend's for their guidance, inspiration and knowledgeable advice throughout the entire period of this work.

Finally, I would like to give a great thanks to University of Gondar for sponsoring this master's program. In addition, special thanks to Bahir Dar University, Bahir Dar Institute of Technology for giving me this education opportunity.

ABSTRACT

Use of carbon fiber reinforced polymer (CFRP) in construction industry is getting better attention. This is partly due to CFRP's superior characteristics such as high strength to weight ratio, Immunity against corrosion and high tensile strength features. A study on application of CFRP in form of grid is rare. Therefore, the present research work presents numerical investigation on use of CFRP grid as a reinforcing material in concrete slab. Experimental result reported in literature (Aljazaeri et al., 2020) was used for validation analysis using ANSYS non-linear finite element software program. Also, analytical formula from ACI was used to verify FE results. Further, parametric study on influential variables such as effect of concrete compressive strength, effect of bottom CFRP grid reinforcement layer and effect of volume fraction of CFRP reinforcement were conducted to get insight into flexural response of CFRP grid reinforced concrete slab.

FEA results indicated that volume fraction of carbon fiber on carbon fiber reinforced polymer reinforcement and concrete grade has effect on structural performance of CFRP grid reinforced concrete. When volume fraction of carbon on CFRP reinforcement increased from control 20% to 30%, 40% and 50%, ultimate load resistance increased by 6.25%, 19.71% and 35.63% respectively. Similarly, when slab concrete compressive strength increased from 56 MPa to 60MPa the ultimate load resistance increased by 6.9% whereas reducing slab concrete strength 56 MPa to 40MP resulted in ultimate load resistance lost by 7.8%.

Key words: ANSYS; Carbon fiber reinforced polymer (CFRP); slab; grid

TABLE OF CONTENTS

LIST OF ABBREVIATIONS

ANSYS	Analysis system
CFRP	Carbon fiber reinforced polymer
CFRPRC	Carbon fiber reinforced polymer reinforced concrete
FRP	Fiber reinforced polymer
GFRP	Glass fiber reinforced polymer
NEFMAC	New fiber material for reinforcing concrete
SRC	Steel reinforced concrete
UHPC	Ultra high performance concrete
USACERL-TR	US Army corporations of engineers' construction engineering research laboratories technical report
WWS	Welded wire steel

LIST OF SYMBOLS

A_f area of FRP reinforcement (mm^2)

a depth of equivalent rectangular stress block (mm)

b width of rectangular cross section (mm)

c distance from extreme compression fiber to the neutral axis

c_b distance from extreme compression fiber to neutral axis at balanced strain

C nonlocal interaction range parameter or neutral axis depth

d distance from extreme compression fiber to centroid of tension reinforcement

D hardening material constant

E_{cm} elastic modulus

f_{bc} biaxial compressive strength of concrete

f'c concrete cylindrical compressive strength

f_f stress in FRP reinforcement in tension (MPa)

f_{fu} design tensile strength of FRP, considering reductions for service environment(MPa)

f_{uc} uniaxial compressive strength of concrete

f_{ut} uniaxial tensile strength of concrete

m Over non-local parameter

M_n nominal moment capacity

mn negative-moment capacity per unit width

mp positive moment capacity per unit width

M_u factored moment

PR_{XY} Poisson's ratio

R_T Tension cap hardening constant

$\alpha 1$ ratio of average stress of equivalent rectangular stress block to f'c

$\beta 1$ is the ratio of the depth of the equivalent rectangular stress block to the depth of the neutral axis.

βc Compression damage evaluation constants

βt Tension damage evaluation constants

γ_{co} Compression damage thresholds

γ_{to} Tension damage evaluation constants

σ_v^c Compression cap parameter

εc strain in concrete

ε_{cu} ultimate strain in concrete

ε_f strain in FRP

ε_{fu} design rapture strain of FRP reinforcement

ρ_b steel reinforcement ratio producing balanced strain condition

ρ_f fiber reinforced polymer reinforcement ratio

φ Strength reduction factor

LIST OF TABLES

LIST OF FIGURES

1. INTRODUCTION

1.1 Background

Structural concrete is usually reinforced with conventional steel bars, without exhibiting any deterioration if it is properly protected from corrosion attack. However, this is not possible in so many cases, such as structures that are exposed to extreme environments in bridge, bridge decks, marine structures, parking and highway structures. In North America, significant temperature fluctuations and the use of deicing salts exacerbate the phenomenon in parking garages and on bridge decks. The combination of moisture contaminated with chlorides and temperature will accelerate the corrosion of steel reinforcement and lead to the deterioration of the structure and eventual loss of serviceability. The corrosion of steel reinforcement in concrete structures is the main factor in reducing the lifespan of these structures. To overcome the corrosion problems and increase the lifespan of reinforced concrete structures a worldwide preferred solution is the use of fiber reinforced polymer (FRP) rebar as an internal reinforcement for concrete structures.

Fiber-reinforced polymer composite reinforcement has been used successfully in many industrial applications and more recently it has been used as concrete reinforcement in bridge decks and other structural elements (Rizkalla, S., and Tadros, G, 1994). FRP composite products were first evolved in the 1950s, starting with temporary structures and continuing with restoration of historic buildings and structural applications. Typical products developed were domes, shrouds, translucent sheet panels, and exterior building panels.

During the late 1970s and early 1980s, many applications of composite reinforcing products were demonstrated in Europe and Asia. In 1986, the world's first highway bridge using composite reinforcing tendons was built in Germany (Taerue, 1993). Since the early 1990's, interest in the use of FRP materials for structures has increased steadily, and there are currently hundreds of field applications of FRPs in structures around the world. In general fiber reinforced polymer (FRP) reinforcement can be used as a potential replacement for steel reinforcement, such as rebar for concrete structures, sheets for flexural and shear strengthening to wrap concrete columns and bridge piers to increase confinement (Saim R, et.al.,2019). Due to the great advantages of the fiber reinforced polymers (FRPs), such as a high strength to

weight ratio, high corrosion resistance and enhanced durability, they have been used as reinforcing materials for concrete structures. A typical application of FRPs is internal reinforcement in concrete slab components. Thus, investigating the structural behavior of CFRP-reinforced concrete member is essential.

In this research a parametric study was conducted to study the influential parameters on the strength and crack propagation of the slab. The parameters such as, concrete compressive strength, bottom CFRP grid reinforcement layer and volume fraction of carbon fiber on carbon fiber reinforced polymer reinforcement were considered. The finite element package ANSYS, mechanical APDL software was used, in which material nonlinearity is considered. The validation of the FE model was done by simulating the experimental work of Aljazaeri et al. (2020) experimental report.

The organization of the thesis is divided into five chapters. The contents of each chapter are presented as follows. Chapter one gives the general introduction, background, statement of the problem, objectives, research significance, scope and limitation of the study. Chapter two includes a review of available literatures on FRP reinforced slabs, historical development of FRP reinforcing materials and application of FRP composites in reinforced concrete structures.

Chapter three presents the details of current thesis work methodology including experimental test details used for validation, finite element analysis procedures (such as element idealization, material models, finite element discretization, loading and boundary conditions)and type of analysis and finite element parametric studies.

Chapter four provides the analysis results and discussions of the behavior of the slab specimens in terms of load-displacement response and crack propagations due to different parameters. Finally; chapter five presents the conclusions based on the findings of the current research and recommendations for future work.

1.2 Statement of the problem

To overcome the corrosion problems and increase the lifespan of reinforced concrete structures, use of carbon fiber reinforced polymer (CFRP) in construction industry is getting better attention. This is partly due to CFRP's superior characteristics such as high strength to weight ratio, Immunity against corrosion and high tensile strength features. A study on application of CFRP in form of grid for internal reinforcement of concrete structures is rare. Therefore, the present research work fills this perceived gap by numerical investigation of CFRP grid as a reinforcing material in concrete slab.

1.3 Objectives of the study

1.3.1 General objectives of the study

The main objective of this thesis is numerical study on flexural performance of CFRP grid reinforced two-way slab system.

1.3.2 Specific objectives of the study

In addition to the general objective, the study aims:

- To investigate the influence of concrete compressive strength on flexural behavior of CFRP grid reinforced two way slab system.
- To study the influence of volume fraction of carbon fiber on carbon fiber reinforced polymer reinforcement on flexural behavior of CFRP grid reinforced two way slab system.
- To investigate the effect of tensile CFRP grid reinforcement layer on the flexural behavior of two-way slab system reinforced with CFRP grid.
- To investigate the combined effect of variables on flexural behavior of CFRP grid reinforced two way slab system.

1.4 Significant of the study

The existing research will help to partners and researchers to understand the flexural performance of CFRP grid reinforced two-way slab system. Also, it will be used for further studies to provide more insight into the behavior of concrete slabs reinforced with FRP grid.

1.5 Scope and limitation of the study

The scope of this thesis is limited to clearly study the flexural behavior of two-way slab systems reinforced with carbon fiber reinforced polymer grid reinforcement. Powerful engineering software, ANSYS (v.20.R2) was used to perform a structural 3D non-linear finite element analysis of RC slab models. This study mainly addressed and limited on numerical investigation of the response of CFRP grid reinforced concrete slab. Experimental results reported from literature for finite element analysis verification (Aljazaeri et al.2020). In this study four parameters such as, concrete compressive strength, bottom CFRP grid reinforcement layer and volume fraction of carbon fiber on CFRP were considered to get insight in flexural behavior of two-way slab system with CFRP grid reinforcing material.

2. LITERATURE REVIEW

2.1 Introduction

This chapter provides a comprehensive review of the literature on the historical development of FRP's as reinforcing material and its use in structural reinforcement on RC structures, FRP composite materials and mechanical properties, flexural behavior of FRP reinforced concrete slab members, numerical investigation of FRP reinforced concrete slab members behavior of FRP RC structures and summary and focus of this study are presented.

2.2 Historical development of FRP's as reinforcing material

Since the 1960s many highway bridges and structures have started to deteriorate due to the corrosion problems of the reinforcing steel as a result of road de-icing salts in colder climates which accelerated the corrosion of the reinforcing steel. Many strive had taken in the past to overcome the corrosion of steel reinforcement such as applying a galvanized coating to the surface of the reinforcing bars, the use of epoxy coated steel reinforcing bars in 1970s and the use of stainless steel. In the late 1960s, the Bureau of Reclamation in the US developed a program for using polymer impregnated concrete but it was not possible to use steel reinforcement with polymer concrete due to the incompatibility in thermal properties. This led Marshall Vega to manufacture glass fiber reinforced polymer as reinforcement bars (ACI440R-96,A.C., 2002).

In the early 1980's, the use of fiber reinforced polymer (FRP) as reinforcement purpose for construction was developed. However, in field of construction, FRP reinforcement was not easily accepted because the cost effectiveness of FRP was inferior to such conventional reinforcing materials of steel. One of the core causes to use a FRP reinforcing material is the realization that the reinforcing steel, both in reinforced and pre- stressed concrete construction, is corrosion prone. This realization obviously prompts the desire to use noncorrosive materials such as FRP, especially in environments where steel has been shown to be vulnerable (Uomoto et al. 2002). During the 1990s and into the new millennium the utilization of advanced polymer composite materials has made large advances in the civil engineering construction field, particularly in the bridge area.

2.3 Application of fiber reinforced polymer Composites in RC structures

Wide spread application of FRP composite materials did not occur until the mid-1980s as evidenced by the first FRP reinforced concrete bridge, built in Germany [American Concrete Institute (ACI) 1995]. The FRP reinforcement has been used successfully in many industrial applications and also has been used in several bridge decks recently constructed in North America. The Morristown Bridge, which is located in Vermont, United States, is a single span steel girder bridge with integral abutments spanning 43.90m (Bonmokrane et.al. 2006).

Fiber-reinforced polymers have a great potential for replacing steel reinforcement in bridges, buildings, and other civil infrastructures (L.C.Hollaway, 2003). The principal reason for selecting these composites is their corrosion resistance, which leads to longer life and lower maintenance and repair costs. The corrosion problem is worst because of deicing salt spread on the bridge road surface in winter months in many parts of the world. The deterioration can become so severe that the concrete surrounding the steel rebar can start to crack and ultimately fall off, thus the structure's load-carrying capacity becomes insufficient. The corrosion problem does not exist with fiber-reinforced polymers.

Fiber-reinforced polymers were also used in slabs in the form of composite grids for instance by [Banthia et al.1995, Rahman et al. 2000, and Yost and Schmeckpeper (2001). CFRP grids have been used as tensile reinforcement in concrete beams, slabs, or bridge decks (Matthys and Taerwe, 2000; Rahman et al. 2000; Yost et al. 2001; Yost and Schmeckpeper, 2001; Zhang et al. 2004). Also, a carbon-fiber reinforced polymer grid can be used as a replacement for steel spirals for confining precast, pre-stressed concrete piles (Hatem et al., 2016).

2.4 FRP composite materials and mechanical properties

Fiber reinforced polymer composites are composed of relatively high strength parallel fibers enclosed in a resin matrix, which serves to bind the fibers into a single structure. The resin matrix provides the means to transfer applied stresses to the fibers and protects the fibers from deleterious interaction from the environment, such as oxidation and corrosion.

Using a layering process, the FRP is formed into rigid two and three - dimensional grid shapes. The most common types of fibers typically used in fiber reinforced

polymers are glass, carbon and aramid. As fiber reinforced polymer (FRP) materials used for reinforcing concrete structures, FRP grids such as carbon fiber reinforced polymer (CFRP) grid as shown in Figure 2-1 below is widely used. CFRP grid is the main focus of this study and used as internal reinforcement for concrete slab structures.

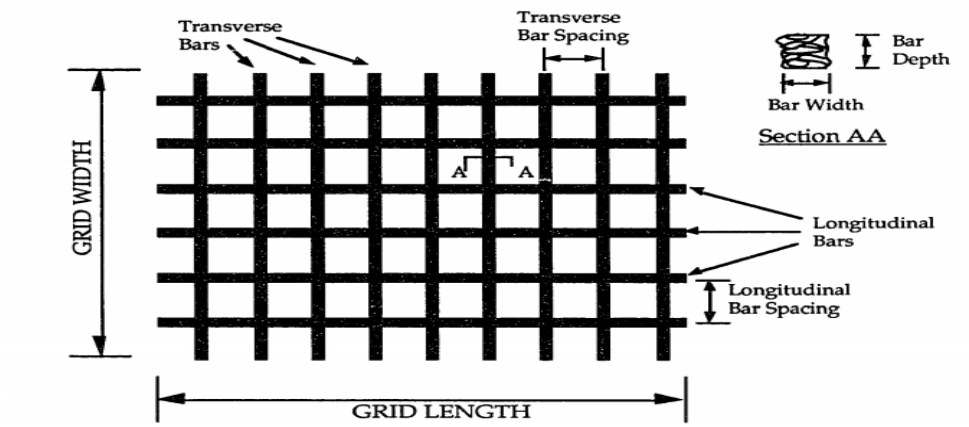

Figure 2-1 Two- dimensional CFRP grid (source: Yost, 1993)

As can be seen from the above figure, a typical 2-dimensional grid consists of intersecting longitudinal and transverse bars. Within a grid, the longitudinal and transverse bars are continuous and orthogonal at their intersection points. The bars are crudely rectangular in shape, possessing smooth top and bottom surfaces and rough fibrous side surfaces (Yost, 1993).

Fiber reinforced polymer materials do not exhibit any plastic behavior, or yielding, before rupture. The tensile behavior of FRP materials consisting of one type of fiber material is characterized by a linear elastic stress-strain relationship until failure; the failure is sudden and occurs without warning. The fibers in FRP material are the main load-carrying and the tensile strength and stiffness of FRP material depends on several factors such as constituent fiber type, fiber orientation, fiber quantity, and method and conditions that the composite is manufactured affect the tensile properties of the FRP material. Stress - strain curve CFRP indicated in Figure 2-2.

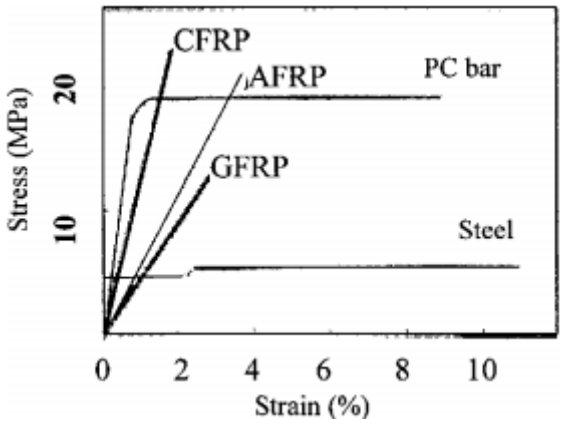

Figure 2-2 Stress -strain relationship of FRP composites and typical reinforcing steel (source: Aljazaeri et al., 2020)

The mechanical properties of fiber reinforced polymer composites are a resultant of the properties of the individual components. The modulus of elasticity for a FRP composite material with a tensile load applied parallel to the longitudinal axis of the fibers is defined by the Volume –fraction rule (Thomas H.Courtney, 1990).

$$Ecomponent = V1 \times E1 + V2 \times E2 \qquad 2.1$$

Where: V1 = volume fraction of component (i) (i.e. percent of gross cross sectional area)

E1= modulus of elasticity of component (i)

Also the stresses in FRP composites are a volumetric weighted average of the stresses in the individual components. The tensile stress in a FRP composite material is defined as:

$$\sigma(component) = V1\sigma1 + V2\sigma2 + ... \qquad 2.2$$

The failure stress of the composites is dependent on the modulus of elasticity and the maximum strain of the fibers which make up the composite.

$$\sigma(component) = E(component) * \varepsilon(component) \qquad 2.3$$

Table 2-1 Tensile Properties of Reinforcing Bars (Source: ACI 440.1R-06)

	Steel *	GFRP*	CFRP*	AFRP*	BFRP**
Nominal yield stress(MPa)	276-517	N/A	N/A	N/A	N/A
Tensile strength(MPa)	483-690	483-1600	600-3690	250-2540	1200
Elastic modulus(GPa)	200	25-51	120-580	41-125	50
Yield strain (%)	0.14-0.25	N/A	N/A	N/A	N/A
Rupture strain (%)	6.0-12.0	1.2-3.1	0.5-1.7	1.9-4.4	2.5

*Typical values for fiber volume fractions ranging from 0.5 to 0.7(ACI440.1R-03)

**Values for fiber volume fraction of 0.8

2.5 ACI Approach on FRP reinforced concrete flexural member

The design of FRP-reinforced concrete members for flexure is analogous to the design of steel-reinforced concrete members. The design of members reinforced with FRP bars should take into account the uniaxial stress-strain relationship of FRP materials. Both FRP rupture and concrete crushing mode of failures are acceptable in governing the design of flexural members reinforced with FRP bars provided that strength and serviceability criteria are satisfied. To compensate for the lack of ductility, the member should possess a higher reserve of strength.

The strength of cross section should be performed based on the following assumption

A. Plane section before loading remains plane after loading (Strain in the concrete and the FRP reinforcement is proportional to the distance from the neutral axis).
B. The maximum usable compressive strain in the concrete is assumed to be 0.003.
C. The tensile behavior of the FRP reinforcement is linearly elastic unit failure.
D. A perfect bond exists between concrete and FRP reinforcement.

The design flexural strength at a section of a member should exceed the factored moment.

$$\varphi Mn \geq Mu \qquad 2.4$$

The nominal flexural strength of FRP reinforced concrete member can be determined based on strain compatibility, internal force equilibrium and controlling strength limit state. Also it is depend on whether it is controlled by concrete crushing or FRP rupture. The controlling limit states can be determined by comparing the FRP reinforcement ratio to the balanced reinforcement ratio, which is the ratio where concrete crushing and FRP rupture occur simultaneously. Because FRP does not yield, the balanced ratio of FRP reinforcement is computed using its design tensile strength. The FRP reinforcement ratio and balanced FRP reinforcement ratios are computed as follow.

$$\rho f = \frac{Af}{bd} \qquad 2.5$$

$$\rho fb = 0.85 \frac{\beta 1 fc'}{fFu} \frac{Ef\varepsilon cu}{Ef\varepsilon cu + fFu} \qquad 2.6$$

The nominal flexural strength of FRP reinforced concrete structures are described below based on the controlling limit states.

1. When ρf > ρfb, the failure of the member is initiated by crushing of the concrete, and the stress distribution in the concrete can be approximated with the ACI rectangular stress block. Based on the equilibrium of forces and strain compatibility.

$$\Rightarrow Mn = A_f * f_f (d - \frac{a}{2}) \qquad 2.7(a)$$

$$a = \frac{A_f f_f}{0.85 f_c' b} \qquad 2.7(b)$$

$$f_f = Ef\varepsilon cu \frac{\beta 1 d - a}{a} \qquad 2.7(c)$$

FRP reinforcement is linearly elastic at concrete crushing failure mode, so the stress level in the FRP can be found from Eq. (2.7c) because it is less than f_{fu}.

2. When ρf < ρfb, the failure of the member is initiated by rupture of FRP bar, and the ACI stress block is not applicable because the maximum concrete strain (0.003) may not be attained. In this case, an equivalent stress block would need to be used that approximates the stress distribution in the concrete at the particular strain level reached.

Here; the concrete compressive strain at failure εc, the depth to the neutral axis (c), the rectangular stress block factors (α1) and β1, are unknown.

Where; α1 is the ratio of the average concrete stress to the concrete strength

β1 is the ratio of the depth of the equivalent rectangular stress block to the depth of the neutral axis.

The analysis involving all these unknowns becomes complex. Nominal flexural strength at a section can be computed as shown in Eq. (2.9a).

$$Mn = As * f_{fu}\left(d - \frac{\beta 1 c}{2}\right) \qquad 2.9(a)$$

$$c = \left(\frac{\varepsilon_{cu}}{\varepsilon_{cu} + \varepsilon_{fu}}\right) d \qquad 2.9(b)$$

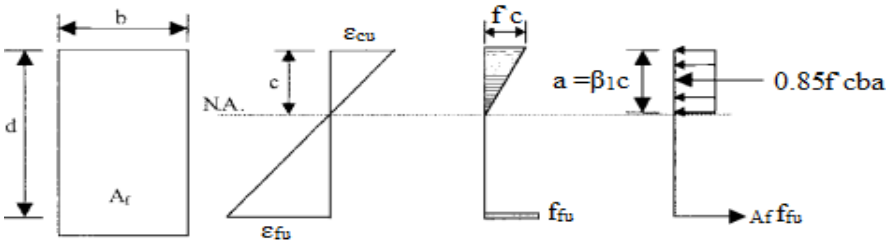

(a) Failure governed by concrete crushing

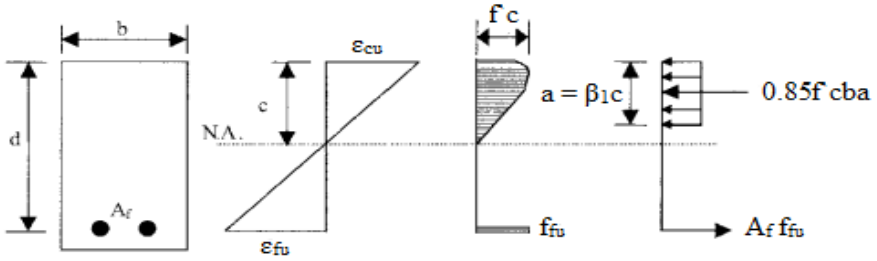

(b) Balanced failure condition

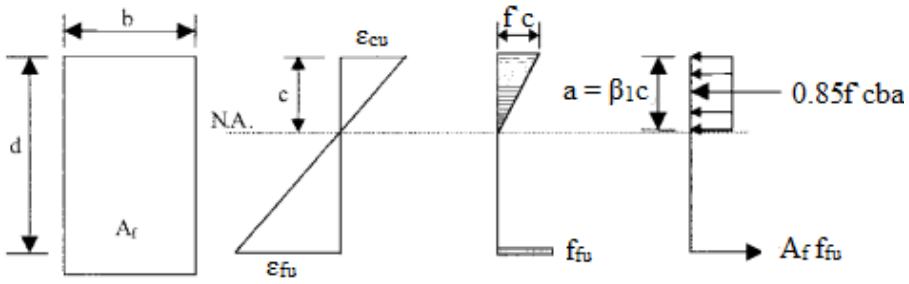

(c) Failure governed by FRP rupture (concrete stress may be nonlinear)

Figure 2-3 Strain and stress distribution at ultimate conditions (source: ACI440-1R-06)

2.6 Flexural behavior of FRP reinforced concrete slab members

AL-Sunna, et al. (2012) studied the deflection behavior of FRP reinforced concrete slabs. A total of 12 GFRP and CFRP RC slabs covering a wide range of reinforcement ratios were investigated. The experimental test program was consisted of three series of GFRP and three series of CFRP tests on RC slabs. The test result indicated that, from samples with high amount of reinforcement could provide better control over the additional deformations (shear or bond-slip induced deformations) at the lower load levels and the additional deflections were observed at the higher load level. It was also concluded that the contribution of shear and bond induced deformations can be of major significance in FRP RC elements having moderate to high reinforcement ratios.

L. Ombres, et al. (2000) investigated the cracking and deflection of FRP reinforced concrete one-way slabs under static loading condition. Four full-scale, reinforced concrete one-way slabs have been tested up to failure. All specimens were tested as simply supported beams subjected to a four-point load. Parameters considered in the analysis include type of reinforcement (steel and FRP), amount and size of FRP rebar and thickness of concrete cover. For the specimen of the conventional reinforced concrete slabs, mode of failure of steel yielding followed by the crushing of concrete was attained and the first crack was initiated at mid-span. Also, it was showed that for specimens of GFRP reinforced concrete slabs, the first crack was initiated at mid-span and was accompanied by a sudden increase in deflection due to stiffness reduction of the specimen. The stiffness of the GFRP reinforced concrete slabs is significantly lower than the steel reinforced members after cracking; resulting is larger crack widths and deflection. Also, the magnitude of mid-span deflection after cracking and the width of the first crack increased as the amount on the reinforcement ratio reduced. But the ultimate capacity of slabs increases with the amount of GFRP rebar.

R. Sivagamasundari and G. Kumaran (2008) conducted an experimental study on the flexural behavior of concrete one-way slabs reinforced with Glass Fiber Reinforced Polymer (GFRP) reinforcements as well as conventional (Steel) reinforcements when subjected to static and repeated loadings. A total number of forty slabs of size 2.4 x 0.6 m were cast, out of which twelve slabs were reinforced with steel reinforcements and the remaining slabs were reinforced with GFRP reinforcements. Twenty numbers of slabs were tested under static loading condition and another twenty numbers of slabs were tested under repeated loading condition. Test parameters such as, two thicknesses (100 and 120 mm), two grades of concrete (M20 and M50), four types of reinforcements (Grooved GFRP, Sand coated GFRP, Plain GFRP and Conventional) and two types of reinforcement ratios provided in longitudinal direction (0.82 and l .15%) were used. From the static test, it was observed that the load-deflection response of GFRP reinforced slabs was linearly up to first cracking and after first cracking; there was a sudden increase in deflection due to the stiffness reduction of slabs. In case of steel slabs, the first crack was initiated at mid span and was accompanied by smaller deflections and crack widths when compared to the GFRP reinforced slabs. Due to the low modulus of and different bond characteristics of the GFRP reinforcements, slabs reinforced with GFRP reinforcements exhibited larger deflections and strains than those reinforced with conventional reinforcements. As the longitudinal reinforcement ratio of slabs increases from 0.82 to 1.15% the ultimate load carrying capacities of GFRP reinforced slab increases from 20-30% and the deflections and crack widths were not that much significant. Similarly, an increase in the grade of concrete from 20 to 30 N mm^2, the slabs result from 15 to 20% increase of ultimate load bearing capacities with insignificant reduction in deflection. By increasing the depth of the slab from 100 to 120 mm, the ultimate static load was increased by 82% and the deflection was reduced by 0.8 times. From the conducted fatigue test it was concluded that GFRP reinforced concrete slabs had a better performance and longer fatigue life when compared to those reinforced with steel. Sand coated GFRP reinforced slabs showed best fatigue performance than the other GFRP reinforced slabs.

Hesham and Mostafa (2020) carried out an experimental and numerical investigation on the flexural behavior of two-way solid slabs reinforced with GFRP bars. All slabs have dimensions of 1750 X1750 mm with clear spans of 1350 x1350m and marginal

beams at the edges of the slabs with dimension of 200x200 mm were used. It was noted that, using GFRP bars as reinforcement for the two-way concrete slabs instead of the traditional steel bars is feasible and reliable since they achieved almost similar physical properties. The numerical models using ANSYS software were achieved almost similar results for the experimental specimens with respect to the cracking pattern, the load displacement relationship, and the load-strain relationship. Crack pattern for slabs reinforced with GFRP bars has better distribution with increasing the reinforcement ratios: GFRP bars in the tested reinforced slabs did not fail in rupture so crushing of concrete forms the mode of failure. Also, increasing the reinforcement ratio and slab thickness increases the ultimate capacity and decreases the max deflection for two way solid slabs reinforced with GFRP bars.

Matthys, S. and Taerwe, L (2000) studied the flexural behavior of FRP grid reinforced concrete slabs under static loading. Eight concrete slabs, reinforced with steel and different types of FRP. The slabs had a width of 1,000 mm; a depth of either 120 or 150 mm, a span of 4 m, and a total length of 4.5 m were used. A normal-strength concrete with 30 MPa was used for all the slabs. The FRP used as reinforcement in six of the eight concrete slabs consisted of NEFMAC grids such as, carbon fibers and a mixture of carbon and glass fibers (hybrid type) were used. The other two slabs were reinforced with, a steel mesh (S500 with a diameter of 10 mm, mesh size 150 mm) consisting of longitudinal and transverse bars. Test results showed that due to the lower modulus of elasticity of FRP, the flexural stiffness in the cracked state turns out to be lower, which results in larger deflections. At a load level of 7 KN (service load of the reference slab), the deflections of the FRP-reinforced slabs are 4 to 5 times higher than reference slab. By increasing the cross-sectional area of the reinforcement (slabs with carbon and hybrid fiber) or by increasing the slab thickness an acceptable deflection, similar to reference slab were obtained. But the use of smaller grid spacing reduced the width and the height of the cracks. Slabs with higher reinforcement area and/or higher slab depth showed much higher ultimate loads.

2.7 Numerical investigation of FRP reinforced concrete slab members

Meng and Khayat (2016) conducted a parametric study on the flexural behavior of the UHPC panels reinforced with embedded Glass fiber-reinforced polymer grids. Three dimensional nonlinear finite element models were developed with ABAQUS. Panels with different geometries and reinforcement configurations were modeled. The model

was compared with the experimental data to validate the model by determining the stress distribution and damage propagation in composite panels. The thin and flexible GFRP grids were modeled by using 2-node linear 3-D truss elements (ABAQUS Element T3D2). Each T3D2 element has 2 nodes, and each node has 3 degrees of freedom. The UHPC matrix, steel rollers, and rubber pad were modeled with 8-node linear 3-D brick reduced integration elements (C3D8R). The nonlinear finite element equations were solved with the Newton Raphson method. The concrete damaged plasticity model was successfully implemented for the characterization of UHPC by using notch beam specimens. The numerical results were in excellent agreement with experimental results (up to 1% error) for the elastic stage that took place before cracking occurred. A greater error (up to 9.5%) can be observed after cracking occurred because the multiple strips in single- or dual-layer FRP grids are assumed to work together perfectly and rupture at the same time in the numerical simulation. parametric studies such as, the effect of panel thickness and reinforcement configuration on peak flexural load, first cracking load, and energy dissipation of reinforced UHPC panels was conducted. For each panel thickness, the panels reinforced with dual-layer GFRP grids exhibited the largest peak load and corresponding mid-span deflection, and the UHPC panels without GFRP exhibited the smallest peak load and corresponding mid-span deflection. The first crack and peak loads can increase with the panel thickness increases. However, no evident difference could be observed for the deflection corresponding to the first crack load and peak load values.

2.8 Summary of previous studies and focus of the study

In general, the use of fiber reinforced polymer reinforcement in the construction industry had got better attention. Because, the fiber reinforced polymer reinforcement have high strength to weight ratio and superior environmental resistance than steel reinforcements. Additionally, studies prove that FRP reinforced concrete slab members have better strength and more economical. Until now few experimental, analytical and FE analysis studies had been conducted on flexural behavior of concrete slab reinforced with FRP grid reinforcement. But further and deep studies are required to examine its behavior under different parameters and to show its better performance. This paper will fill a literature gap and numerically investigated the flexural behavior of FRP grid reinforced slab. The variables considered on this study

are concrete compressive strength, CFRP grid reinforcement layer and volume fraction of carbon fiber on carbon fiber reinforced polymer reinforcement.

3. METHODOLOGY

3.1 Introduction

The method adopted in this study is nonlinear finite element analysis. It was carried out using ANSYS, Mechanical APDL 2020 R2 software program and also used to validate a model and conduct parametric studies on CFRP grid reinforced two way slabs. This software is used to simulate 3D models of non-linear finite element analysis of reinforced concrete two way slab specimens. It is used to model total of sixteen slab specimens including one validated model specimen. The main aim of this chapter is to present all the necessary information's used for non-linear finite element analysis of ANSYS software. The geometrical specification (both experimental and FEA model), element idealization, material models, finite element discretization, loading and boundary condition, and also type of analysis are presented.

3.2 Experimental test details used for validation

3.2.1 Geometrical and material specification of tested slab

The model verification was based on the experimental work carried out in (Aljazaeri et al.2020). In this study, a specimen that was studied in Aljazaeri et al. (2020) was modeled here to show the validity of the implemented ANSYS (v.20.R2) finite element analysis. Then after by using validated model specimens which included the influential parameters on flexural behavior CFRP grid reinforced slab were modeled.

The necessary geometrical data and material properties of reinforcements for modeled specimen are discussed in detail below on the tables (Aljazaeri et al. 2020).

Table 3-1 Geometrical description of the slab (source: Aljazaeri et al. 2020)

Geometry of the slab	Dimensions (mm)
Longer span (length)	1150

Shorter span (width)	1150
Thickness of slab	100
Grid spacing	30mm by 30mm
Concrete cover	20mm

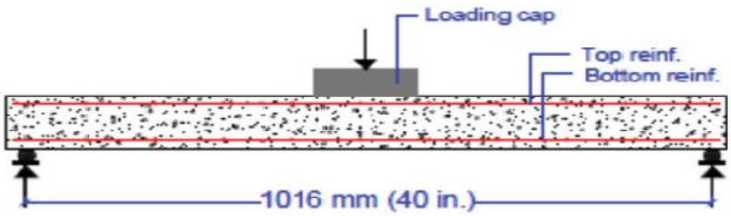

Figure 3-1 Slab geometry and loading points (source: Aljazaeri et al., 2020)

Figure 3-2 Two-way slab system under testing (source: Aljazaeri et al., 2020)

Table 3-2 Characteristics of the reinforcement (source: Aljazaeri et al., 2020)

Reinforcement type	Direction	Cross-section area, mm^2	Yield strength, MPa	Tensile strength, MPa	Elastic modulus, MPa
CFRP grid	Transverse	9.0	NA	496	67,570
	Longitudinal	7.2	NA	393	55,850
WWM steel wire	Transverse	26.5	510	648	180,677
	Longitudinal	28.4	596	634	160,076

Table 3-3 Material properties of concrete (source: Aljazaeri et al. 2020)

Compressive strength	56MPa
Modulus of elasticity	33960 MPa
Poisson ratio	0.2

3.3 The finite element analysis procedure

Finite element analysis procedure includes element idealization; define material properties, meshing, boundary condition, analysis type, loading and solution setting. In order to simulate the actual behavior of a specimen accurately, all its components such as concrete slab, steel grid and CFRP grid have to be modeled properly. In the analysis, choosing of element type and mesh size are important and building the model to provide accurate results with a reasonable computational time.

3.3.1 Element idealization

In this section, for three type of materials used for this study finite element analysis element idealization are presented. The element idealization that has been adopted for concrete, steel and CFRP reinforcement are described as follows.

I. Element type for Concrete

In this study, concrete has been idealized using CPT215 element. It is a 3-D eight-node brick element. The reason to use this element is that it supports the coupled plasticity damage micro-plane model which was used to model nonlinear behavior of concrete material. CPT215 is capable in modeling coupled physics phenomena such as structural pore fluid diffusion, thermal analysis and structural implicit gradient regularization using a nonlocal field. The element geometry is shown in Figure 3-1 and defined by eight nodes and may have the following degrees of freedom at each node:

- Translations in the nodal x, y, and z directions
- Pore-pressure (PRES)
- Temperature (TEMP)
- Nonlocal field values (GFV1, GFV2)

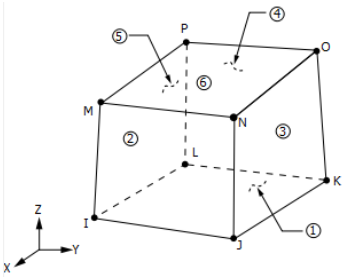

Figure 3-3 CPT215 structural solid geometry (source: ANSYS user manual release 2020)

Before modeling the reinforcement of the slab, the concrete slab, loading plate and support plate were meshed with SOLID185 element since it has the ability to create bond between the concrete and the reinforcement. After the reinforcement is modeled, SOLID185 element is deleted and replaced by its counterpart element that can support the micro-plane model which is by CPT215 element type. However, the temperature and pore-pressure degree of freedom are ignored in this analysis. CPT215 has elasticity, stress stiffening, large deflection, and large strain capabilities. To prevent volumetric mesh locking CPT215 uses selective reduced integration (B bar method). It replaces volumetric strain at the Gauss integration point with the average volumetric strain of the elements.

II. Element type for Reinforcement

Reinforcing CFRP and steel rebar have been idealized using REINF264 element. This element is suitable for simulating reinforcing fibers with arbitrary orientations. Each fiber is modeled separately as a spar that has only uniaxial stiffness. The nodal locations, degrees of freedom, and connectivity of the REINF264 element are identical to those of the base element. REINF264 has plasticity, stress stiffening, creep, large deflection, and large strain capabilities. The figure 3-4 shows the geometry, node locations and normal direction for the element. The element is defined by eight nodes (I, J, K, L, M, N, O, and P).

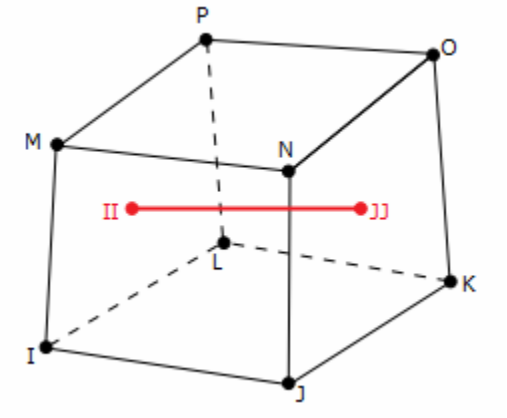

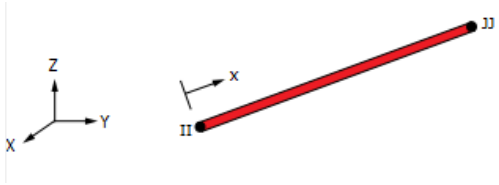

Figure 3-4 (a) Geometry of REINF264 element; (b) REINF264 coordinate system (source: ANSYS user manual release 2020)

Discrete reinforcing method has been used and it is suitable for modeling fibers placed sparsely, or fibers with non-uniform properties, such as cross-section area, material, spacing, and orientation. The reinforcing elements interact with base elements and they have common nodes. In reinforcement section, mesh type pattern has also been used and the advantage of using this pattern is that the orientation of the discrete reinforcing steel is similar to one of the specified element edges.

3.3.2 Material Models

I. Material Model for Concrete

Various computational models for concrete were formulated within different frameworks and focusing on different aspects. The most common approaches are using plasticity theory, continuum damage mechanics or combination of both. The damage mechanics can be used to model the nucleation and growth of cracks whereas the plasticity theory used to model plastic flow of deformation.

In this study, coupled damage-plasticity micro-plane model has been used for modeling concrete material. The model is suitable for simulating engineering materials consisting of various aggregate compositions with differing properties (for example; concrete modeling, in which rock and sand are embedded in a weak matrix of cement), granular material and clay compaction. The model has been developed by (Zreid, I. & Kaliske, M., 2018). The advantage of using this model is to overcome the numerical instability and pathological mesh sensitivity problem causes due to strain-softening materials such as the micro-plane model are susceptible. To overcome these problems, an implicit gradient regularization model has been used. It enhances a nonlocal field that adds two extra degrees of freedom per node.

The coupled damage-plasticity micro-plane model requires 15 parameters which are categorized into four main groups and described as follows;

A. Elasticity

a. Modulus of elasticity, *E* and
b. Poisson's ratio, υ

The modulus of elasticity of concrete was calculated using empirical equation given on equation 3.1.

$$Ecm = 4700\sqrt{fc} \qquad 3.1$$

B. Plasticity

a. Drucker-Prager yield function
   - Uniaxial compressive strength, f_{uc} and its range $f_{uc} \geq f_{ut}$
   - Biaxial compressive strength, and it's range $f_{bc} \geq f_{uc}$
   - tensile strength, and it's range $f_{ut} \geq 0$

These strength parameters; and are common concrete material properties and may be found experimentally. In the absence of testing data, the following empirical relations as shown in equation (3.2) and (3.3) can be used:

$$fbc = 1.15 * fcu \qquad 3.2$$

$$fut = 1.4\left(\frac{fuc}{10}\right)^{2/3} \qquad 3.3$$

The compression cap parameters σ_v^c (intersection point abscissa between compression cap and Drucker-Prager yield function) and R (ratio between the major and minor axes of the cap) can be calculated as follows:

$$\sigma_V^C = \frac{-2 * fbc}{3} \qquad 3.4$$

$$R = \frac{Xo}{f1} * \sigma_V^C \qquad 3.5$$

C. Damage

To identify the hardening parameters (D and R_T) and damage parameters (βc, βt, γ_{co} and γ_{to}), cyclic tests are necessary. These parameters are related, as their interaction controls the softening and the unloading slope. A uni-axial cyclic compression test identifies the parameters D, βc and γ_{co} similarly, a uni-axial cyclic tension test identifies the parameters R_T, βt and γ_{to} and. In the absence of uni-axial cyclic tension tests, R_T=1 and $\beta t = 1.5\,\beta c$ can be used as starting values. The tension damage threshold γ_{to} is often set to zero, as softening in tension starts almost immediately after the elastic limit. The over-nonlocal averaging parameter m is a numerical parameter, where m > 1 regularizes the solution. Typically m is taken as 2.5 (ANSYS user manual release 2020).

Generally, coupled damage-plasticity micro-plane model requires 15 parameters; which are the elasticity, plasticity, damage and nonlocal parameters. Table 3-1 gives the parameters and there values used in micro-plane model of the concrete in this research.

Table 3-4 Parameters and their values used for micro-plane model of the concrete

Parameter type	Parameter subtype	Parameter	Range	Values used in the model
Elasticity	-	E_{cm}		33960MPa
	-	Nu		0.2
Plasticity	Drucker-Prager yield function	f_{uc}	$f_{uc} \geq f_{ut}$	56 MPa
		f_{bc}	$f_{bc} \geq f_{uc}$	64.4MPa
		f_{ut}	$f_{ut} \geq 0$	0 Mpa
	Hardening	R_T	$R_T \geq 0$	1
		D_x	$D \geq 0$	45500

	Compression cap	σ_v^c	$\sigma_v^c =$ 1.3* fcu	-30 MPa
		R	R ≥0	2
Damage	Tension Damage evolution constant	βt	$\beta t \geq 0$	8000
	Compression damage evaluation constants	βc	$\beta c \geq 0$	5000
	Tension damage thresholds	γ_{to}	$\gamma_{to} \geq 0$	0
	Compression damage thresholds	γ_{co}	$\gamma_{co} \geq 0$	2e-5
Non local	Nonlocal interaction range	c		100000
	Over nonlocal averaging	m		2.5

II. Material model for CFRP and steel reinforcement

Plasticity is used to model materials subjected to loading beyond their elastic limit. Metals and other materials such as soils often have an initial elastic region in which the deformation is proportional to the load, but beyond the elastic limit a non-recoverable plastic strain develops. Several constitutive models for plasticity are provided to simulate elastic-plastic material behavior. The models range from simple to complex. The choice of constitutive model generally depends on the experimental data available to fit the material constants (ANSYS help, 2020).

The steel reinforcement material was modeled with bilinear isotropic hardening (BIH) of rate independent plasticity using Von Misses type of yield criterion which is applicable for metals. It is described by a bilinear stress versus strain curve. Isotropic hardening causes a uniform increase in the size of the yield surface and results in an increase in the yield stress. This type of hardening can model the behavior of materials under monotonic loading and elastic unloading.

Two linear graphs with slope are used to describe the material properties as shown on Figure 3.4. The initial slope of the curve is the elastic modulus of the material. Beyond the yield stress, plastic strain develops and stress vs. total strain continues along a line with slope defined by the tangent modulus (ET). The tangent modulus cannot be less than zero or greater than the elastic modulus (ANSYS help, 2020). Four parameters are required to define the elasto-plastic behavior of steel reinforcement; which are the elastic modulus and Poisson's ratio which defines the elastic behavior; the tangent modulus and yield stress which defines the plastic behavior.

The CFRP reinforcement was modeled as an isotropic elastic material. The input data that was used to model the steel and CFRP grid is given on table 3-5.

Table 3-5 Mechanical properties of CFRP grid and steel reinforcement (source: Aljazaeri et al., 2020)

Reinforcement type	Direction	Modulus of elasticity (MPa)	Yield strength (MPa)	Poisson's ratio
CFRP grid	Longitudinal	E_X=55,850	NA	PR_{xy}= 0.3
	Transversal	Ex= 67,570	NA	PR_{xy}= 0.3
WWM	Longitudinal	Ex= 180,677	596	PRxy= 0.3
Steel wire	Transversal	Ex= 160,076	510	PRxy=0.3

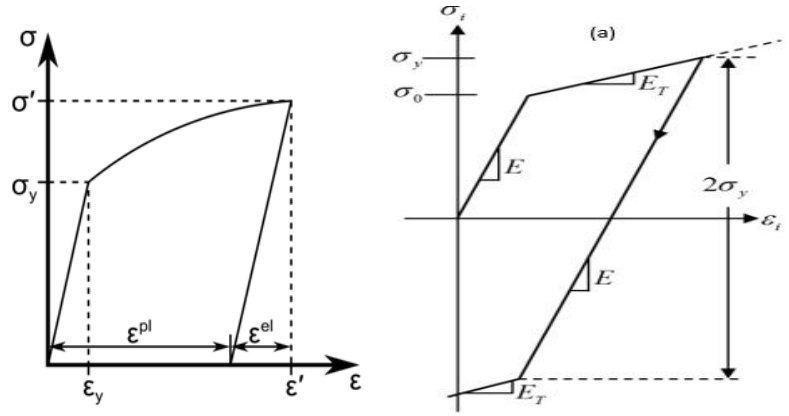

(a) (b)

Figure 3-5 (a) Stress-strain curve for an elastic plastic material: (b) stress vs. total strain for bilinear isotropic hardening (source: ANSYS user manual release 2020).

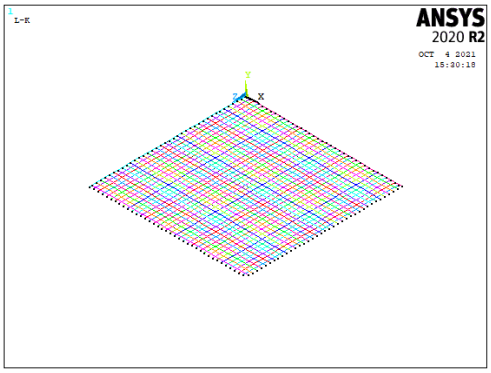

Figure 3-6 CFRP grid reinforcement modeling

3.3.3 Finite Element Discretization

As an initial step, a finite element analysis requires meshing of the model. In other words, the model is divided into a number of small elements, and after loading, stress and strain are calculated at integration points of these small elements (Bathe, 1996). In this study, the concrete, loading plate and supporting plate were meshed with eight node brick element (hexahedral mesh). The validated model has a total of 1297 elements 1768 nodes. Before meshing each model was assigned with an element type which used to model the behavior of the slab under that given loading condition, material type and section type if available. All of these properties are called mesh attributes. To get good result the use of square mesh has been suggested, as shown in Figure 3-7.

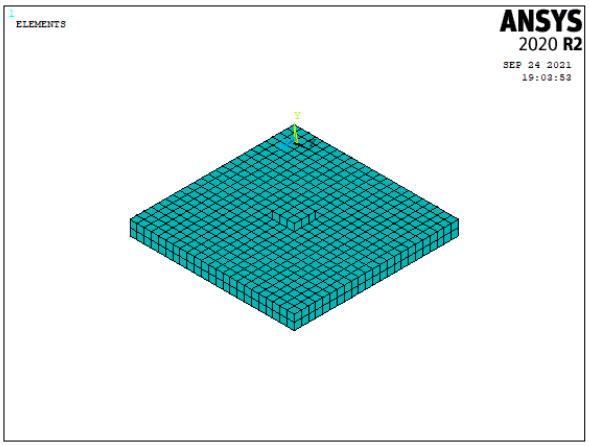

Figure 3-7 Meshing of finite element analysis model

An important step in finite element modeling is the selection of the mesh density. On FEA model using ANSYS a fine mesh is recommended, particularly at probable damage-prone regions. But in this study to obtained mesh-independent results, the mesh size may need to be less than the half of square root of the nonlocal parameter(c). A convergence of results is obtained when an adequate number of elements are used in a model. Therefore, in this finite element analysis modeling an appropriate mesh density of 50mm has been used.

3.3.4 Loading and boundary conditions

Loads can be applied either on solid models (key points, lines, hard points or areas) or finite element models (nodes and elements). Wherever the loads are applied on the model, the solver or the program automatically transfers them to nodes and elements at the beginning of the solution.

Displacement boundary conditions are needed to constraint the model to get a unique solution for each finite element analysis model. In this study one edge support was modeled by restricting three transition degree freedoms in x, y and z direction and the other three edge support was modeled by restricting degree of freedom in y direction. The maximum displacement load was applied at a height of 150mm which is 23 mm in the negative Y direction. The loading and boundary conditions for FEA model specimens are shown in Figure 3-8.

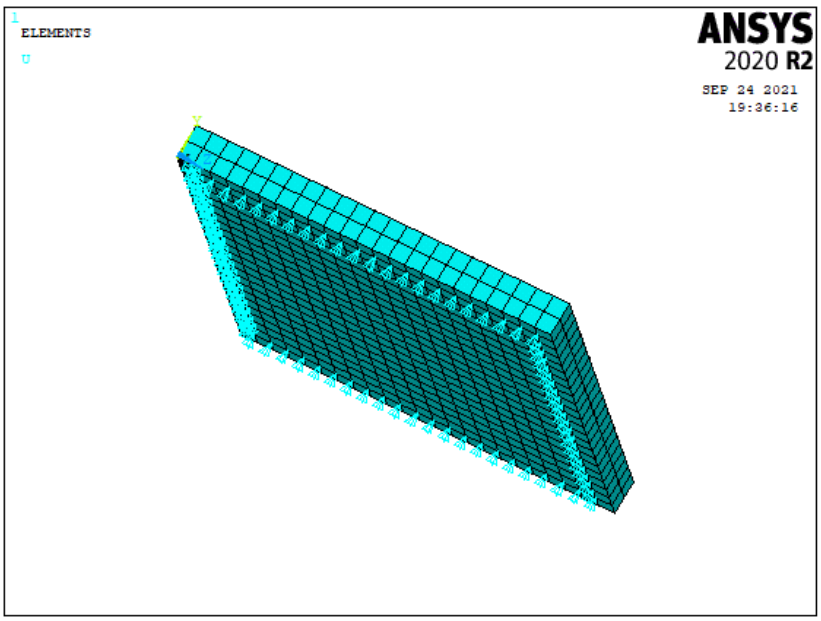

Figure 3-8 loading and boundary conditions.

3.3.5 Type of Analysis

In nonlinear analysis, the total load applied to a finite element model is divided into a series of load increments called load steps. At the completion of each incremental solution, the stiffness matrix of the model is adjusted to reflect nonlinear changes in structural stiffness before proceeding to the next load increment. In this structural analysis, the nonlinear finite element analysis has been performed using ANSYS software. Newton-Raphson equilibrium iteration has been used to solve nonlinear problem in ANSYS software of incremental load analysis. In order to predict the nonlinear behavior, the load applied to a finite element model has been subdivided into a series of load increments which can be applied over several load steps. Newton-Raphson equilibrium iterations in a single-degree-of-freedom nonlinear analysis are illustrated in Figure 3-9. Before each solution, the Newton-Raphson method evaluates the out-of-balance load vector, which was the difference between the restoring forces (the loads corresponding to the element stresses) and the applied loads. The program then performs a linear solution, using the out- of balance loads, and checks for convergence. If convergence criteria are not satisfied, the out of-balance load vector is reevaluated, the stiffness matrix is updated, and a new solution is obtained. This iterative procedure continues until the problem converges.

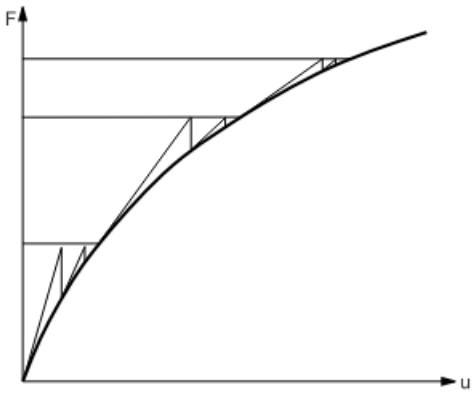

Figure 3-9 Newton-Raphson approach

The challenging situation during the analysis is getting reasonable sub-steps used for a defined load step. Increasing the sub-step improves the accuracy of the solution but takes more computational time to complete the solution and decreasing the sub-step may make the analysis dynamic (apply large load at a time) and gives error results; it also cause errors like element formulation errors. To solve such problems ANSYS have automatic time stepping feature to optimize the task of obtaining solution with

reasonable accuracy and time. When using automatic time stepping, if a solution fails to converge within a sub-step, the bisection method is activated, which restarts the solution from the last converged sub-step. The automatic time steeping was on during the analysis. It is used to determine the time step size and the applied loads automatically in response to the current state of the analysis under consideration. There are two important features of the automatic time stepping algorithm. The first feature concerns the ability to estimate the next time step size based on the current and past analysis conditions and make proper load adjustment. The second feature of automatic time stepping is the time step bisection component when the solution did not converge. Its purpose is to decide whether or not to reduce the present time step size and redo the sub-step with a smaller step time (ANSYS user manual release 2020).

3.4 Finite element parametric studies

Parametric study was conducted on three variables of CFRP grid reinforced two-way slab. The variables of study and models of parametric studies are mentioned below.

3.4.1 Variables of parametric Study

A. Compressive strength of concrete: 40Mpa, 56MPa and 60Mpa.
B. Tensile reinforcement layer: one layer and two layers.
C. Volume fraction of carbon fiber, 20%, 30%, 40%, and 50%

In this study, one of the specimen was conducted as control specimen and parametric study on the above three variables of study was conducted on the remaining CFRP grid reinforced slab specimens. The parametric study model specimens with combination of study variables are shown in Table 3-6. The specimen designation CFRPRC-C56-1-20 is described as follows. The first label (‘‘CFRPRC’’ indicates Carbon fiber reinforced polymer reinforced concrete slab), second label (‘‘C56’’ indicates concrete compressive strength of 56MPa), third label (‘‘1’’ indicates CFRP layer which is one and the fourth label (‘‘20’’ indicates the volume fraction of carbon fiber in CFRP is 20%).

Table 3-6 parametric study model specimens with combination of variables.

		Variables combination

Parameter	Specimen	Concrete compressive strength(MPa)	Tensile CFRP grid layer	Volume fraction of carbon fiber (%)
Concrete compressive strength (MPa)	SRC-C56-1-20	56	1	20
	CFRPRC-C56-1-20	56	1	20
	CFRPRC-C40-1-20	40	1	20
	CFRPRC-C60-1-20	60	1	20
Volume fraction of carbon fiber (%)	CFRPRC-C56-1-20	56	1	20
	CFRPRC-C56-1-30	56	1	30
	CFRPRC-C56-1-40	56	1	40
	CFRPRC-C56-1-50	56	1	50
	CFRPRC-C60-1-40	60	1	40
CFRP grid Layer	CFRPRC-C56-2-20	56	2	20

4. RESULTS AND DISCUSSIONS

4.1 Introduction

In this chapter the FE analysis results that were used for validating the experimental test and the parametric studies are presented. Ultimate load carrying capacity and concrete damage of the slab are the results used for verification of FE model. Three variables are considered to conduct the parametric study. The slab that was used for validation is also used as a reference specimen for the parametric study. The results are presented in terms of load- displacement relationship, ultimate load carrying capacity and concrete damage.

4.2 Mesh Sensitivity Study

Mesh size affects the accuracy of the results and the computational time. To get optimum element size, sensitivity analysis should be conducted and it was conducted in this study by taking different mesh sizes until good result with relatively small analysis time is obtained. Also conducted until getting an accurate solution to that of an experimental test results. In this study 50mm, 25mm and 20mm mesh sizes were considered. The 50mm mesh size decrease the computational time and gives good result within the elastic region but, it over estimate the result on softening. On the other hand, 20mm and 25mm mesh size highly increases the computational time and

difficult to know the results beyond the yield point. The flexural load-displacement curves obtained from the FE analysis for the mesh sizes considered and the experimental result are plotted on the graph presented on figure 4.1

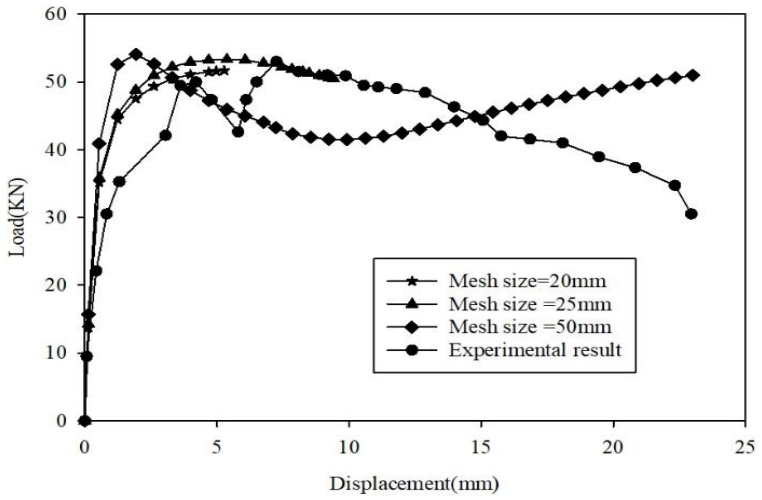

Figure 4-1 Mesh sensitivity study in FEA result

4.3 Validation results of the finite element model

In this section, non-linear finite element analysis results used for validation test discussions are presented in terms of load - displacement relationship, ultimate load carrying capacity and concrete damage.

4.3.1 Load - Displacement Relationship and ultimate load capacity

The deformation of the specimen is represented by the maximum vertical displacement of the slab at loading location. The yield point; where the load-displacement curves for the FE analysis to be non-linear at load around 23KN. After yielding the nonlinear load displacement relation is observed and reached ultimate load resistance of 54.1481KN. Similarly the yield point from experimental load - displacement curves occurs at load around 22KN. After yielding point; the nonlinear load displacement relation is observed and reached ultimate load resistance of 53KN. The ultimate load resistance of FE analysis and the experimental results shows good agreement with a minimum variation of ultimate load carrying capacity. The percentage error is 2.12%. Also it is calculated by dividing the absolute value of the difference between the experimental result and FE result by the experimental result.

Table 4-1 Accuracy of FE analysis results in terms of ultimate load resistance

Ultimate load carrying capacity(KN)				
Experimental result	FE result	Analytical result	Percentage error from experimental result	Percentage error from analytical result
53	54.1481	58.56136	2.12%	8.15%

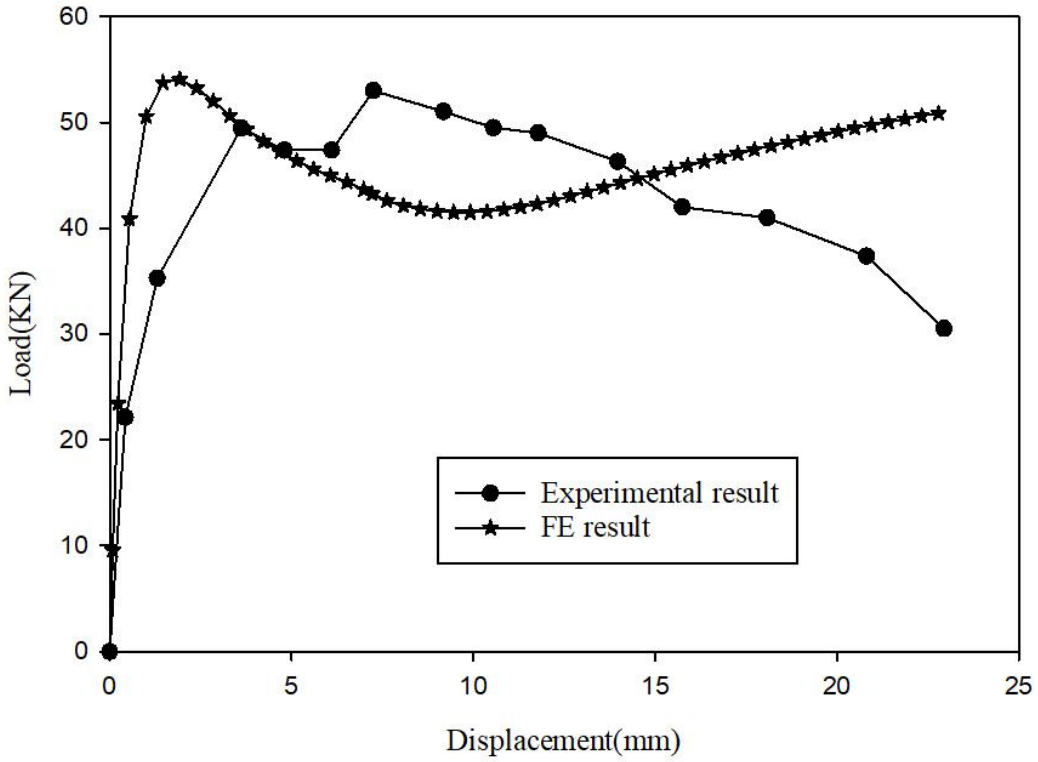

Figure 4-2 FEA & experimental values load-displacement curves

To know the effectiveness of CFRP grid reinforcement in the flexural behavior of slab comparison of the ultimate load resistance of WWS and CFRP grid reinforced slab were conducted. The ultimate load resistance of CFRP grid reinforced slab shows good agreement WWS reinforced slab by minimum error 4.4%. In this regard CFRP grid reinforcement used as replacement of WWS performs well.

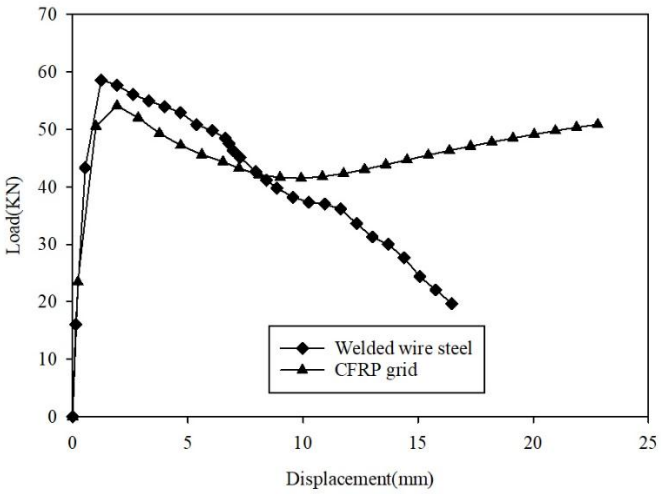

Figure 4-3 load- displacement curves for the FE analysis results with different reinforcement

4.3.2 Concrete Damage

Concrete damage is governed by the stresses in the coupled damage plasticity micro-plane model. This damage is represented by area of regions with various colors. The blue color which represents regions with almost negligible damage: red color which represents highly damaged regions: others which represent small damaged regions. Also the color shows both the magnitudes and distributions of damages. According to the coupled damage plasticity micro-plane model, homogenized total damage is assumed as the main output parameter. Taking into this consideration, a minor crack was first initiated at the center of specimen and propagates to the surface of the slab on both the experimental test and FE analysis. It is shown clearly on figure 4-4.

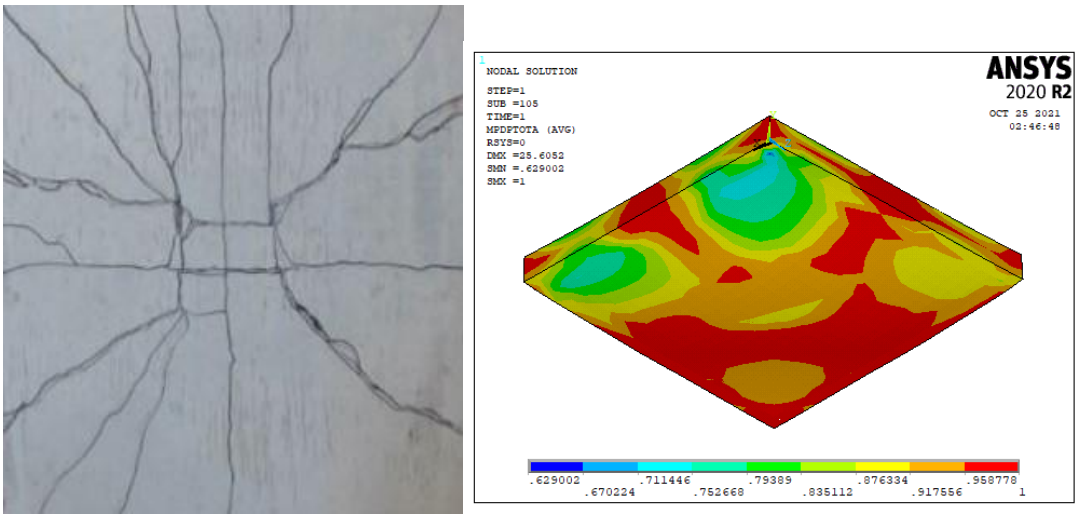

(a) Bottom surface crack pattern experimental result (b) FEM

Figure 4-4 Damage of the concrete in the validation of CFRPRC slab tested by Aljazaeri et al. (2020)

Prediction of crack propagation within the present finite element analysis is depicted as shown in Figure 4-4(b). This crack line prediction which is indicated by orange color area of region of slab can be compared with the observed crack line in the experiment as shown in Figure 4-4(a). There is relatively good agreement between these two figures of crack propagation.

4.4 Finite element parametric study

This section presents the finite element findings and discussions of parametric investigations. The parameters considered include compressive strength of concrete, bottom CFRP reinforcement layer and volume fraction of carbon fiber on carbon fiber reinforced polymer reinforcement. Also the effect of each parameter and their combinations on the flexural behavior of CFRP grid reinforced concrete slab discussions is presented.

4.4.1 Effect of compressive strength of concrete

The effect of compressive strength of concrete (f'c) is an important parameter for the behavior of CFRPRC slabs. This section compares the flexural behavior of CFRP RC slabs with different concrete compressive strength. Concrete normal compressive strength of 40 MPa and high compressive strength of 60 MPa were considered. Figure 4-5 presents the variation in the load-displacement response of CFRPRC slab with different concrete compressive strength. The load-displacement relation before cracking was linear and after cracking up to ultimate load was mainly non- linear. After the peak point the strength and stiffness of the slab were decreased gradually. Based on the load displacement response it can be mentioned that increasing the concrete compressive strength increases the cracking and ultimate load as it could be seen from in Figure 4-5. It occurred due to the fact that concrete members with higher strength need higher tensile strength in reinforcement to conserve equilibrium in the section. Slab with concrete compressive strength of 40MPa (CFRPRC-C40-1-20) decreases the ultimate capacity by 7.79% compared to the control slab specimen (CFRPRC-C56-1-20) whereas, slab with concrete compressive strength of 60MPa (CFRPRC-C60-1-20) increases the ultimate load capacity by 6.9%.

Table 4-2 Comparison of ultimate load capacity of slabs with different concrete compressive strength

Specimens	Concrete compressive strength (MPa)	Ultimate load (KN)	Reduction in ultimate load capacity (%)	Increase in Ultimate load capacity (%)
Control				
CFRPRC-C56-1-20	56	54.1841	-	-
CFRPRC-C40-1-20	40	50.2662	7.79	-
CFRPRC-C60-1-20	60	58.2024	-	6.9

The load –central displacement response of slab with different concrete compressive strength is shown in figure 4-5.

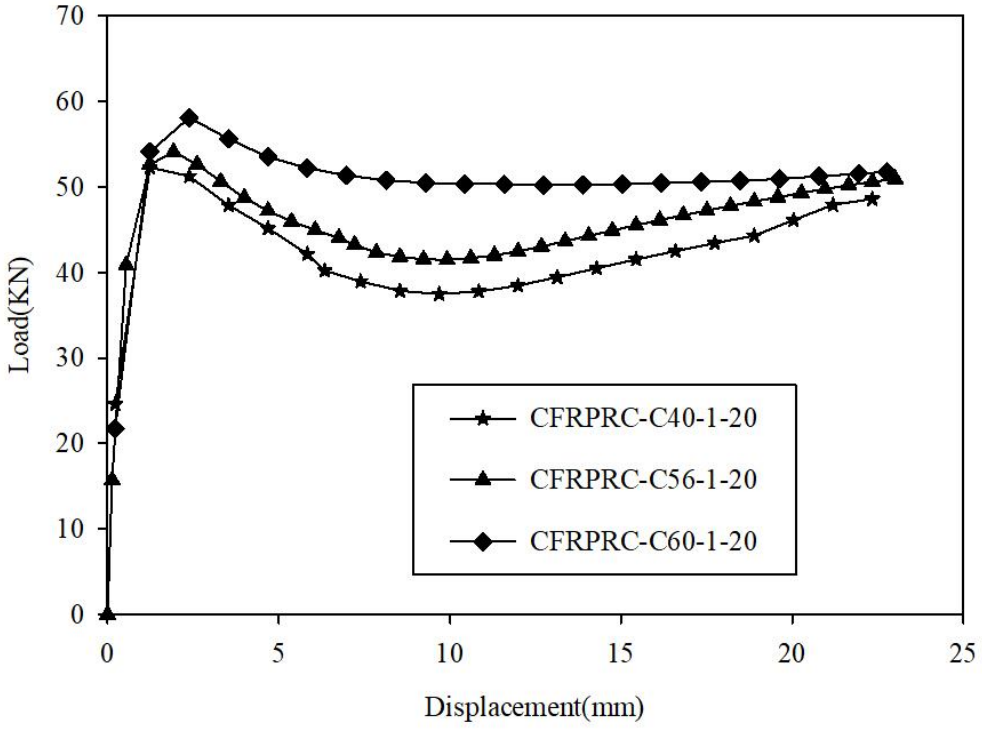

Figure 4-5 Effect of different concrete compressive strength on flexural load capacity of slab

The distribution of stress in slab with concrete compressive strength of 60MPa shows some variation. There is a stress concentration at the center and corner of the slab with

concrete compressive strength 0f 40Mpa, in this regard the high strength of concrete compressive strength have advantages to limit crack propagation over normal strength of concrete.

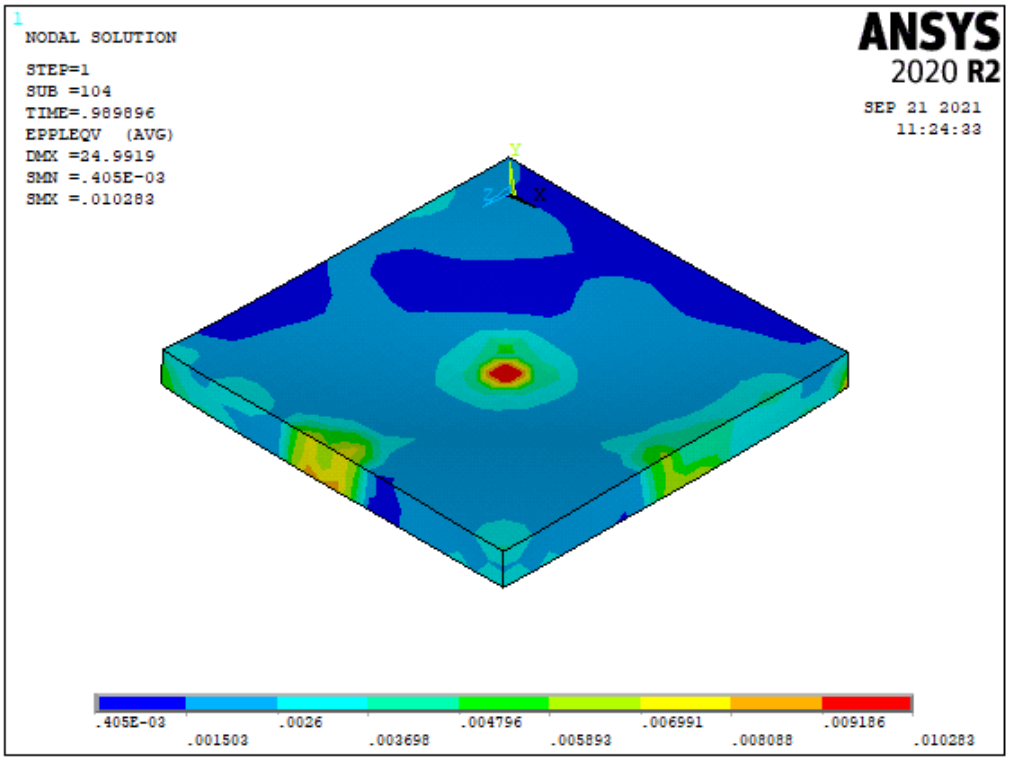

(a) Equivalent plastic strain with 40MPa

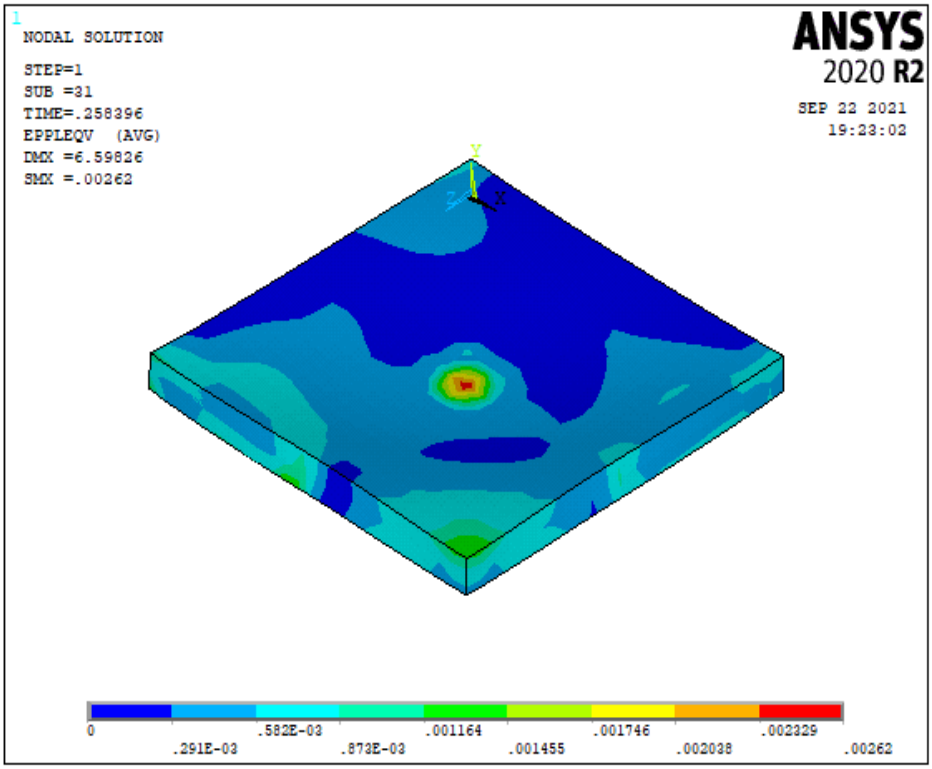

(b) Equivalent plastic strain with 60MPa

Figure 4-6 Equivalent plastic strain with different concrete compressive strength

The damage in the concrete represents micro cracking spread over the large zone, while the plasticity represents the micro crack emerging at the center of damage zone.

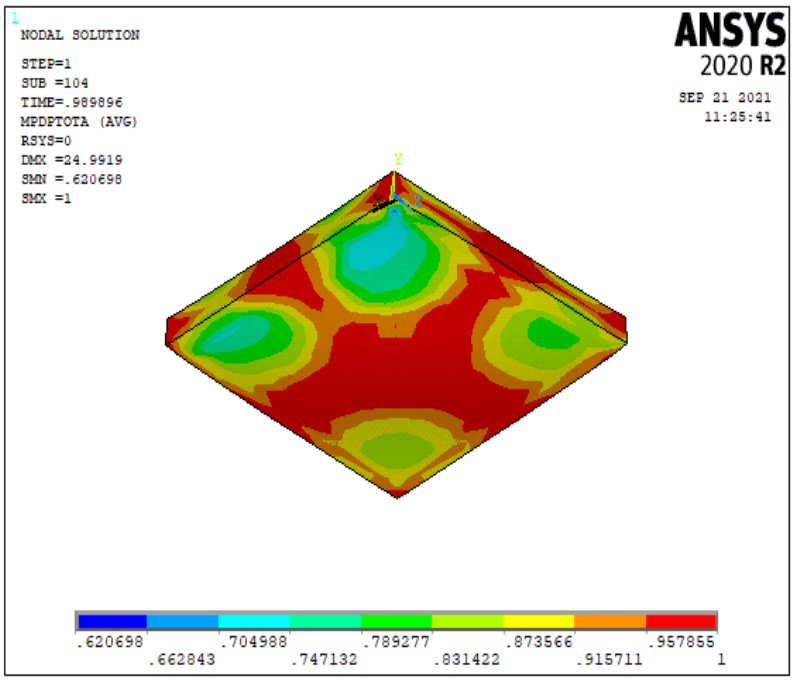

(a) Bottom surface total damage with 40MPa

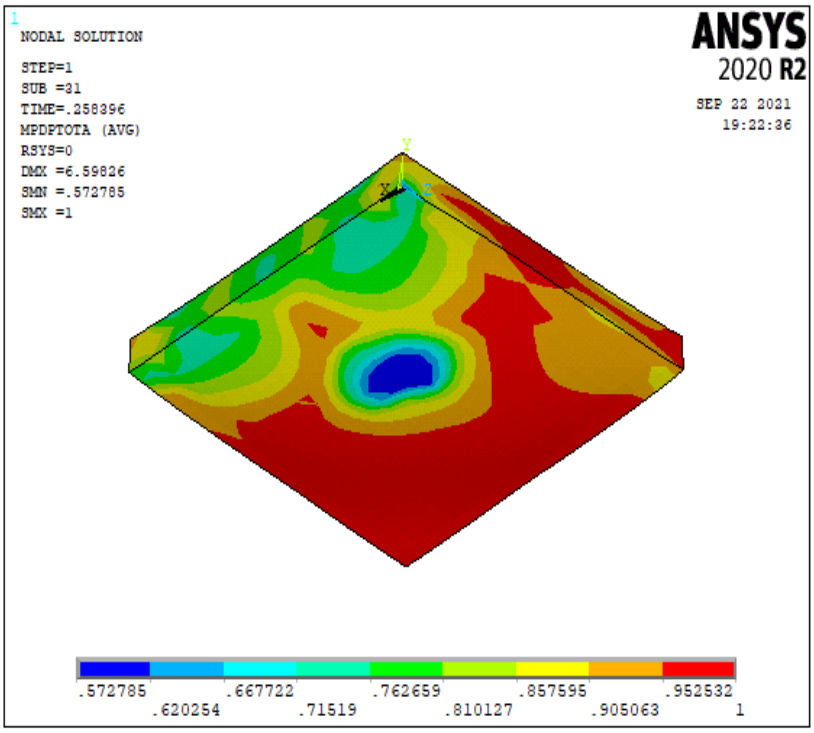

(b) Total damage with 60MPa.

Figure 4-7 Total damage of concrete in the slab with different concrete compressive strength

The homogenized total damage plots of the concrete in both slabs with concrete compressive strength of 40MPa and 60MPa shows that concrete around the bottom surface face of slab. Slab with 40MPa is highly damaged than the concrete at the same location of the slab with 60MPa.The area of undamaged blue color region for slab with 60MPa is high.

4.4.2 Effect of tensile CFRP grid reinforcement layer

This section compares the behavior of CFRPRC with different layers of tensile CFRP grid reinforcement with the same concrete compressive strength and volume fraction of carbon fiber on CFRP slab specimens. Two CFRP grid reinforcement layer (1-layer and 2-layers) were considered to assess the effects on the flexural behavior of CFRPRC slabs. The load- displacement curves for each specimen are developed by taking a node at the top of the slab where maximum vertical displacement is observed. Figure 4-8 presents the variation in the load-displacement response of slab with different CFRP grid reinforcement layer. Based on figure 4-8, it can be mentioned that increasing CFRP grid reinforcement layers increases the ultimate load capacity. It

occurred due to the fact that increasing the reinforcement ratio on concrete members increases the ultimate load capacity. Slab with double layer of CFRP grid reinforcement (CFRPRC-C56-2-20) increases the ultimate capacity by 29.4% compared to the control slab specimen (CFRPRC-C56-1-20).

Table 4-3 Comparison of ultimate load resistance of slabs with different CFRP reinforcement layer

Specimens	CFRP grid reinforcement layer	Ultimate load capacity(KN)	Increase in ultimate load capacity (%)
CFRPRC-C56-1-20	1	54.1841	-
CFRPRC-C56-2-20	2	76.7815	29.4

The load –central displacement response of slab with different concrete compressive strength is shown in figure 4-8.

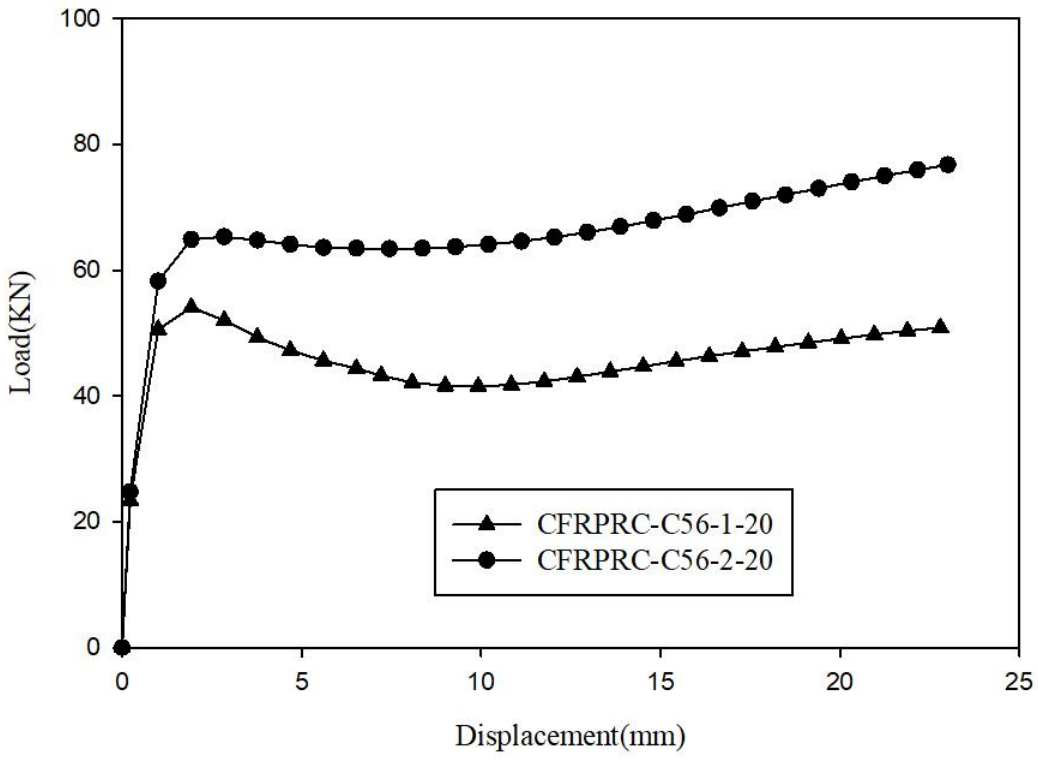

Figure 4-8 Effect of bottom CFRP grid reinforcement layer on flexural load capacity of slabs

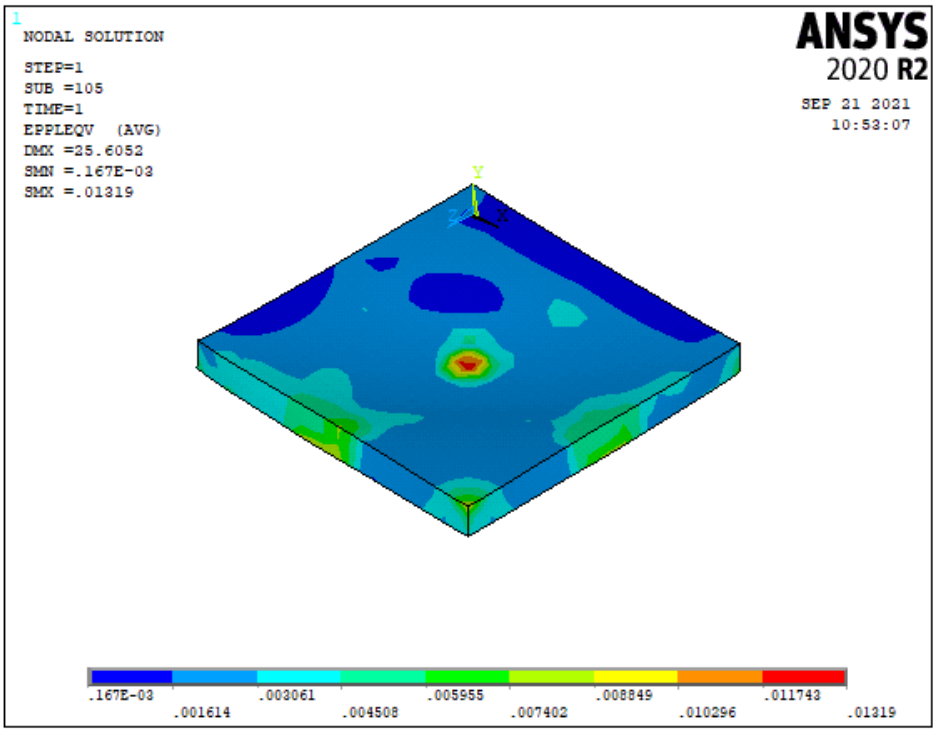

(a) Equivalent plastic strain with 1-layer

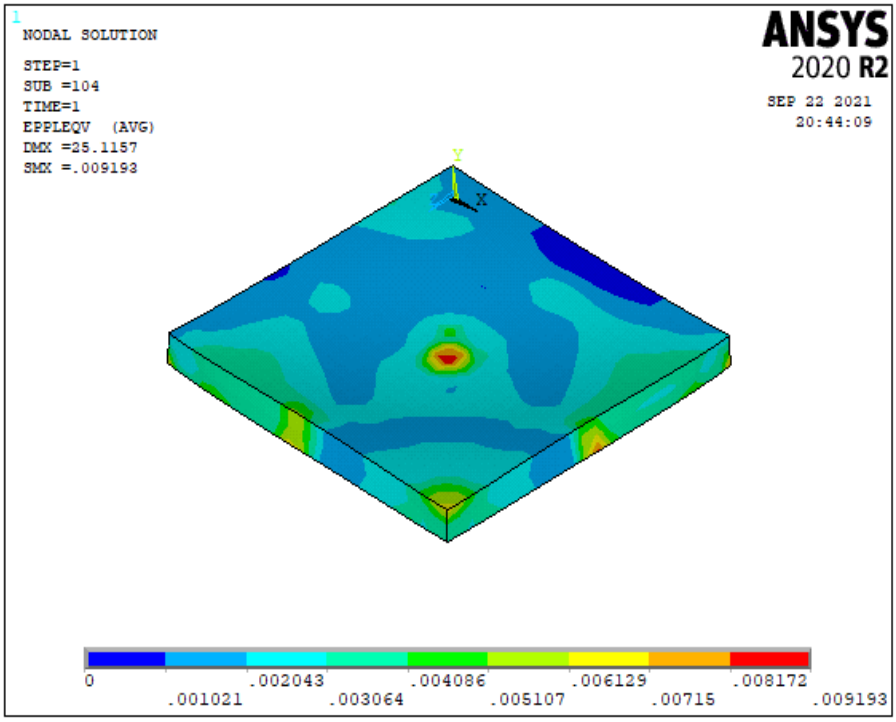

(b) Equivalent plastic strain with 2-layer

Figure 4-9 Equivalent plastic strain with different CFRP grid layer

The distribution of stress in slab with two CFRP grid layer shows some variations and it is better than slab with one CFRP grid layer. The observed color shows the magnitude and distribution of scalar damage variable defined in coupled damage plasticity micro-plane model. The homogenized total damage plots of the concrete in both slabs with 1 CFRP grid layer and 2 CFRP grid layer shows that concrete around the bottom surface of slab shown in figure 4-10. The damage observed on concrete of slab reinforced with 1CFRP grid layer covers larger area. Whereas the concrete damage observed on slab reinforced with 2 CFRP grid layer covers small area and the distribution is better. Also the crack propagation is very well. In this regard double layers of grid reinforcement have advantages to limit crack propagation.

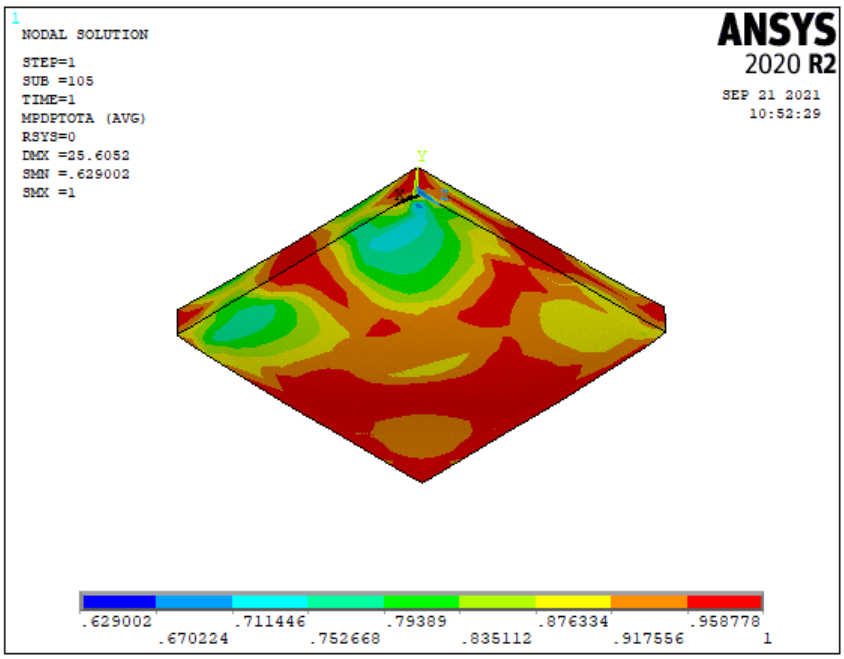

(a) Total damage with 1-layer

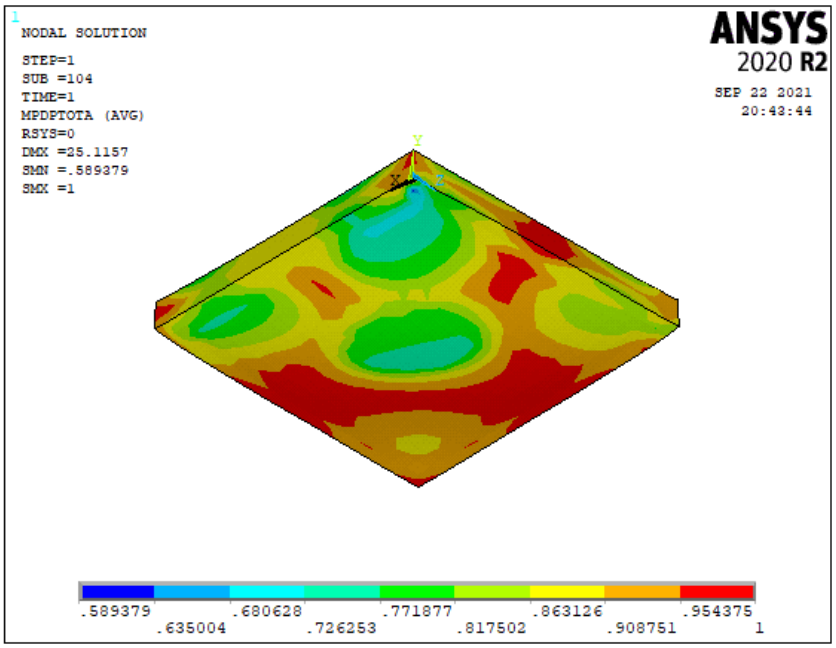

(b) Total damage with 2-layer

Figure 4-10 Damages of concrete in slab with various bottom CFRP grid reinforcement layer

4.4.3 Effect of Volume fraction of carbon fiber in CFRP

This section compares the behavior of CFRP RC slabs with different volume fraction of carbon fiber specimens. Four volume fraction of carbon fiber (20%, 30%, 40% and 50%) were considered to assess the effects on the flexural behavior of CFRP-RC slabs. Figure 4-11 presents the variation in the load-displacement response of slab with different volume fraction of carbon fiber of CFRP grid reinforcement. Based on the load displacement response it can be mentioned that increasing the volume fraction of carbon fiber increases the ultimate load capacity as it could be seen from in Figure 4-11. It occurred due to the fact that the reinforcing fiber in CFRP provides the strength and stiffness to the composite and generally carries most of the applied loads. So, increasing the volume fraction of fiber in carbon fiber reinforced polymer reinforcement tends to get better ultimate load capacity of carbon fiber reinforced polymer reinforced concrete structures. Slab with 50% of carbon fiber in CFRP grid reinforcement (CFRPRC-C56-2-50) increases the ultimate load capacity by 35.63% compared to the control slab specimen (CFRPRC-C56-1-20). Slab with 30% and 40% of carbon fiber in CFRP increases the ultimate load capacity by 6.25% and 19.71% than control slab with 20% of carbon fiber in CFRP respectively.

Table 4-4 Comparison of ultimate load resistance of slabs with different volume fraction of carbon fiber on CFRP

Specimens	Volume fraction of carbon on CFRP (%)	Ultimate load capacity(KN)	Increase in ultimate load capacity (%)
CFRPRC-C56-1-20	20	54.1841	-
CFRPRC-C56-2-30	30	57.7988	6.25
CFRPRC-C56-1-40	40	67.488	19.71
CFRPRC-C56-1-50	50	84.1731	35.63

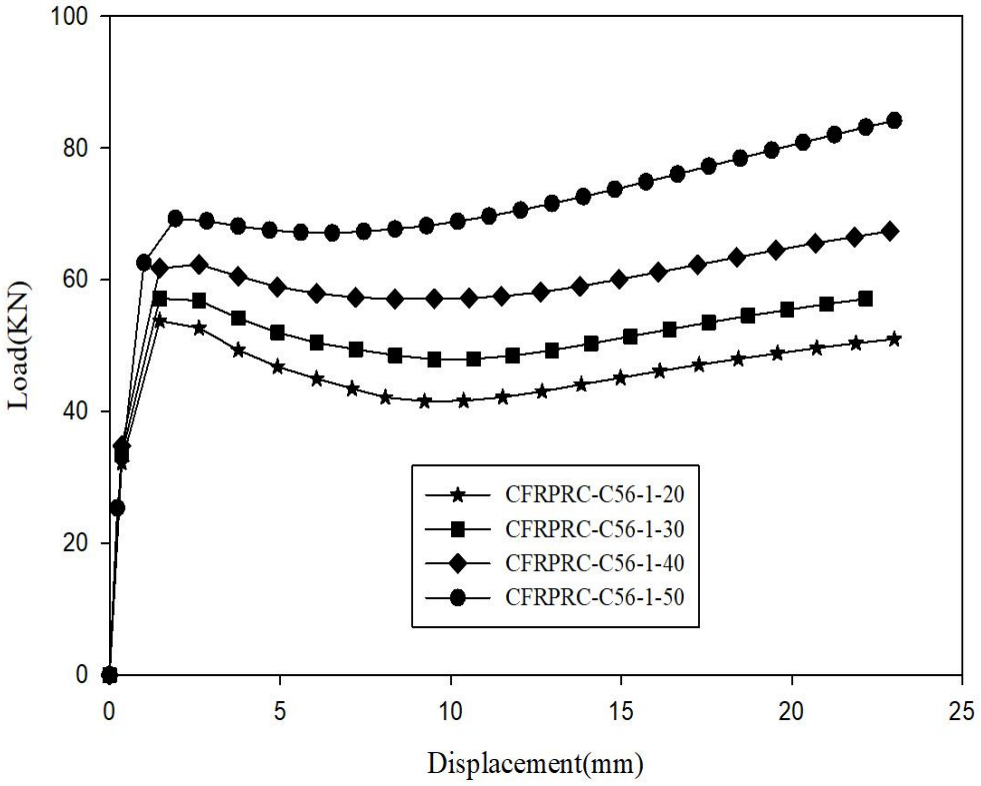

Figure 4-11 Effect of different volume fraction of carbon fiber on flexural load of slabs.

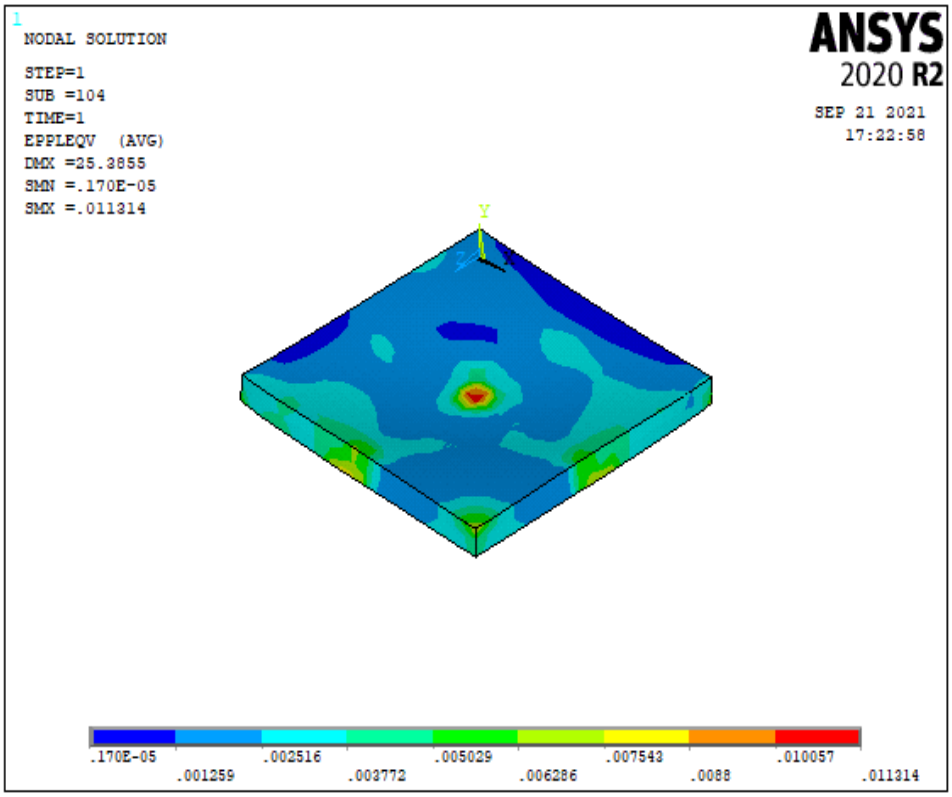

(a) Equivalent plastic strain with 30%

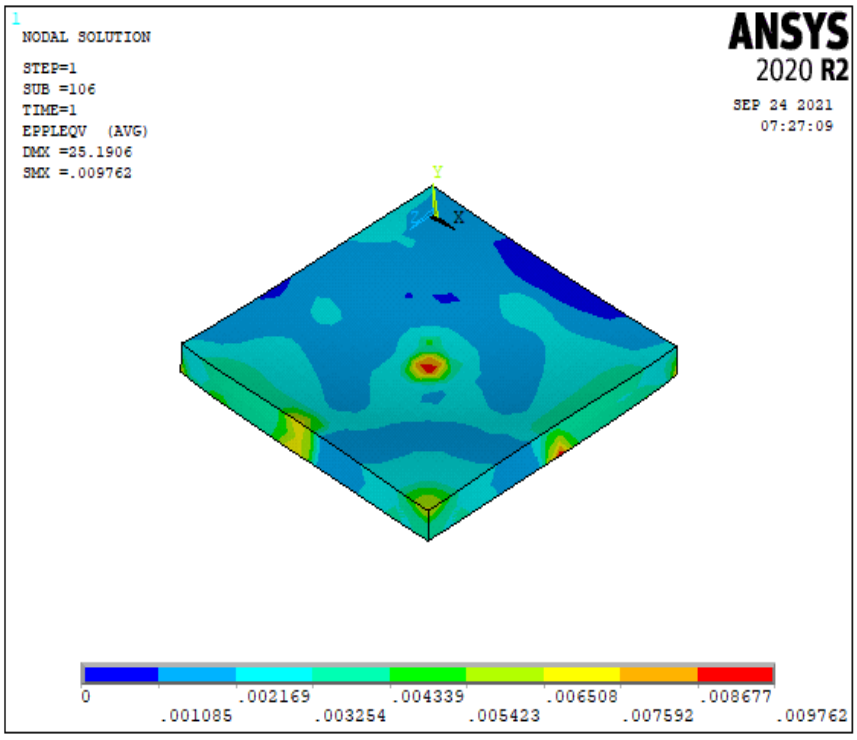

(b) Equivalent plastic strain with 40%

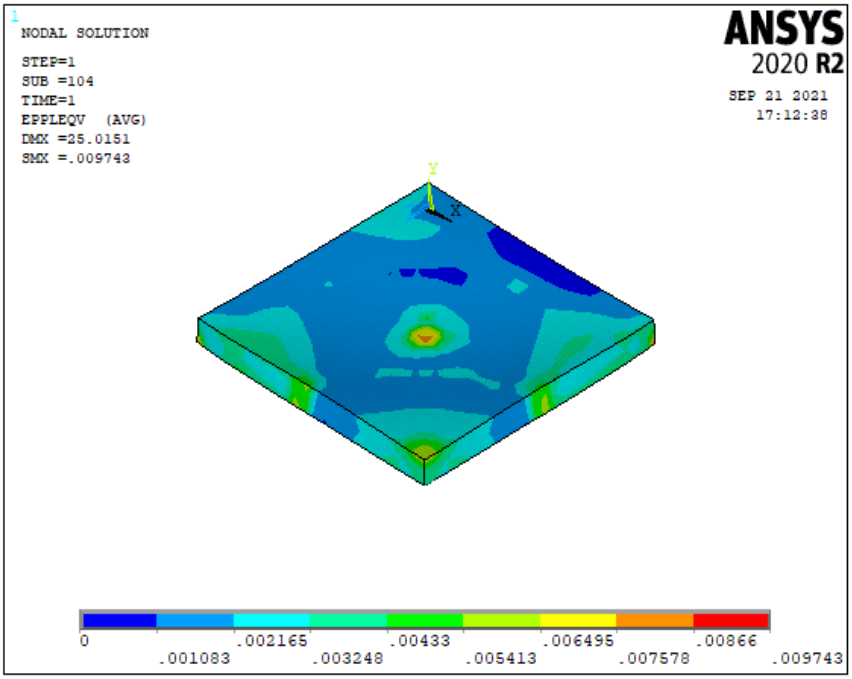

(c) Equivalent plastic strain with 50%

Figure 4-12 Equivalent plastic strain with various carbon fiber fraction of CFRP reinforcement

In micro plane modeling, the damage and cracking behavior can be expressed in terms of concrete tensile and compressive damage. Under this section effect of volume fraction of carbon fiber on carbon fiber reinforced polymer reinforcement on the failure mode of slab is discussed by considering micro plane homogenized total damage as main output parameter. As mentioned on figure 4-12 the slab with high volume fraction of carbon fiber on CFRP reinforcement shows that the damage of the concrete covers a smaller area and has a better distribution. Whereas the damage observed on the concrete of low volume of carbon fiber CFRP grid reinforced slab covers larger area and the distribution is concentrated on edge of concrete.

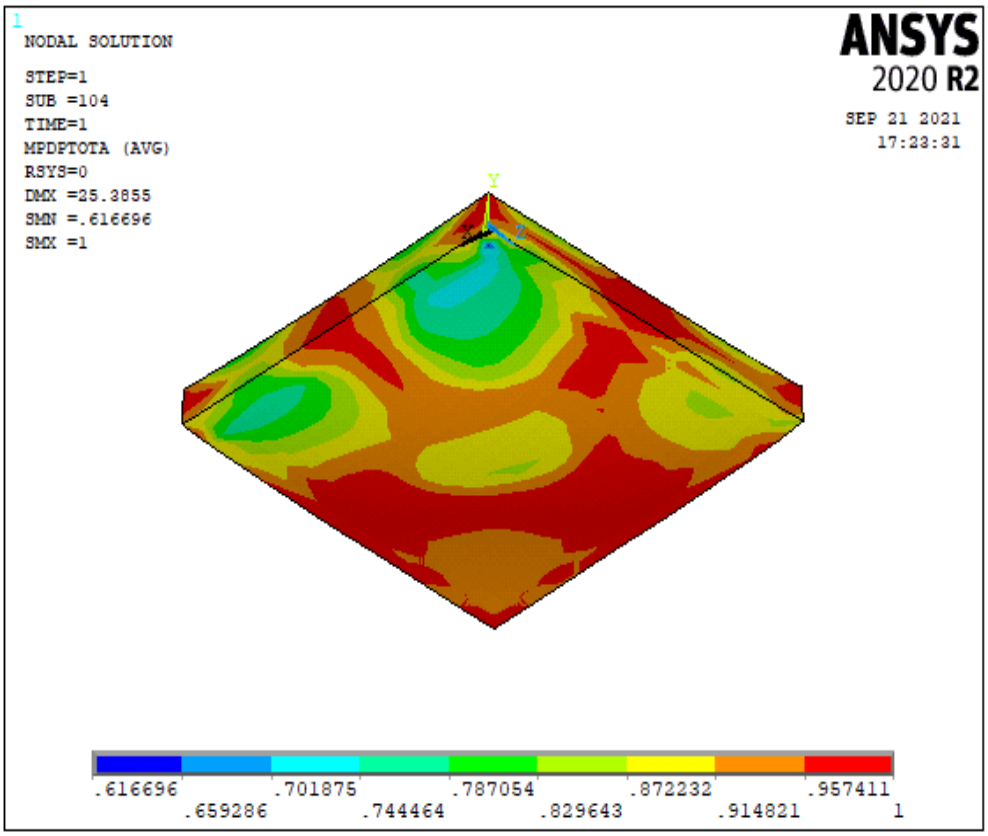

(a) Total damage with 30%

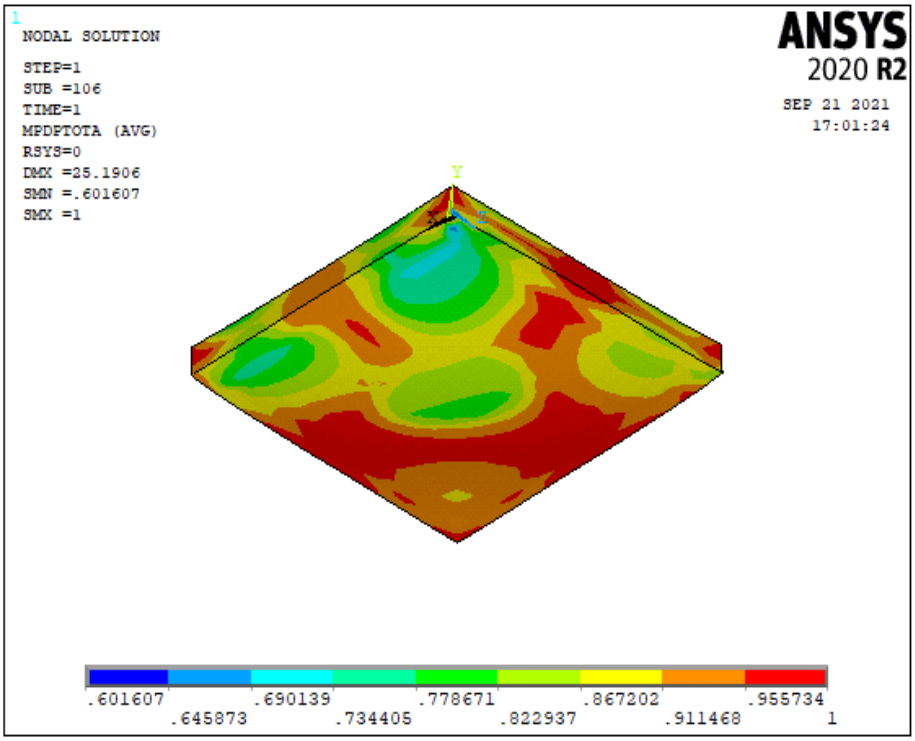

(b) Total damage with 40%

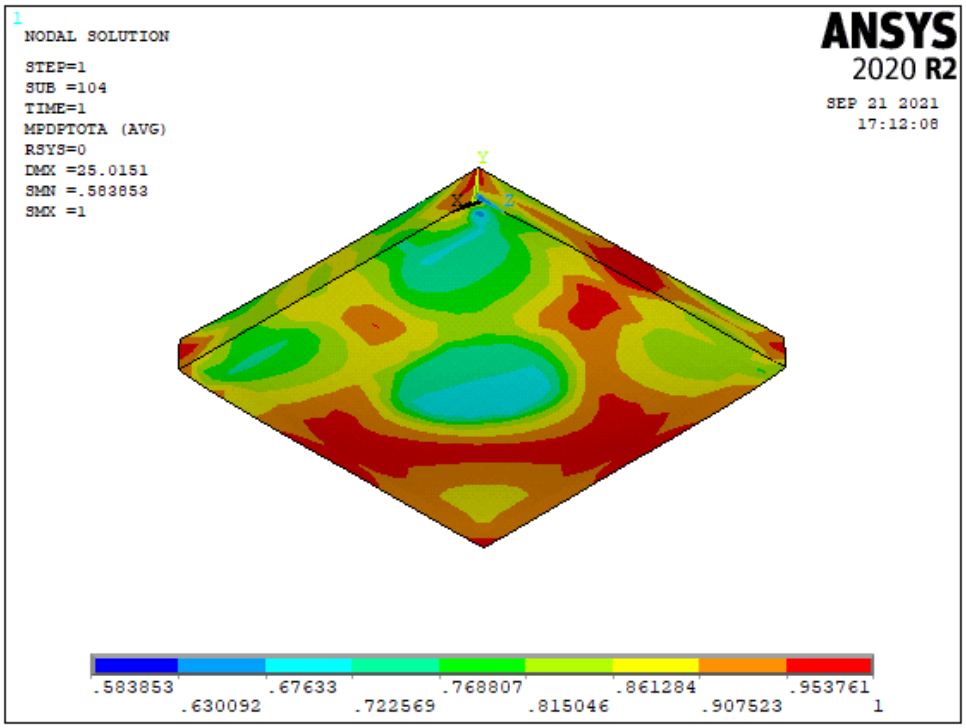

(a) Total damage with 50%

Figure 4-13 Damages of concrete in slab with various volume fraction of carbon in CFRP grid reinforcement

Ductility

Ductility measures the plastic deformation of reinforced concrete members. Also it is the property that enables them to sustain loads when strained beyond their elastic limit. It is calculated using the ratio of maximum displacement to yielding displacement in a load displacement curve for CFRP grid reinforced concrete slabs

$$\mu = \frac{\Delta u}{\Delta y} \qquad 4.1$$

Where: Δu displacement at failure and Δy displacement at yield.

Table 4-5 Ductility ratios of CFRP grid reinforced slab at different volume fraction of carbon fiber on CFRP

Volume fraction of carbon on CFRP (%)	Δy(mm)	Δu(mm)	$\mu = \frac{\Delta u}{\Delta y}$
20	2.15385	23	10.679
30	2.61385	23	8.799

40	3.30385	23	6.962
50	3.99385	23	5.759

From the above table the volume fraction of carbon increases the values of ductility ratio for CFRP grid reinforced concrete slab is decreased. This shows that when the carbon content on CFRP bar increased, it increases the strength of reinforcement in addition increases the resistance of CFRP reinforced slab. Due to this reason the ductility of CFRP grid reinforced slab decreased. Also it shows that the failure of a member is decreased and it has a good resistance.

4.4.4 Combined effect of Variables

This section compares the behavior of CFRPRC with combination of variables. Based on concrete compressive strength, two groups were considered to assess the effects on the behavior of CFRPRC slabs. The first group used a concrete compressive strength of 40Mpa and the second group used 60MPa. Figure 4-14 presents the variation in the load-displacement response of CFRPRC slab. Based on group 1 specimens of the load displacement response it can be mentioned that slab with normal strength of concrete and high volume fraction of fiber in CFRP performs very well. Hence the ultimate load capacity of CFRPRC-C40-1-30 is increases by 13.5% than CFRPRC-C56-1-20 whereas the ultimate load capacity of CFRPRC-C40-1-40 is increases by 23.61%. Similarly, based on group 2 specimens of the load displacement response it can be mentioned that the ultimate load capacity of CFRPRC-C60-1-30 is reduced by 12.23% than CFRPRC-C56-1-50 whereas the ultimate load capacity of CFRPRC-C60-1-40 is almost similar with CFRPRC-C56-1-50 with minimum error 2.12%. In this regard volume fraction of carbon fiber has significant effect than concrete in the ultimate load capacity of CFRPRC slab.

Table 4-6 comparison of ultimate load resistance of slabs with combination of two variables

Specimens	Volume fraction of carbon on CFRP (%)	Ultimate load capacity(KN)	Increase in ultimate load capacity (%)	Reduction in ultimate load capacity (%)

CFRPRC-C56-1-20	20	54.1841	-	-
CFRPRC-C40-1-30	30	62.71	13.5	-
CFRPRC-C40-1-40	40	70.93	23.61	-
CFRPRC-C56-1-50	50	84.1731	-	-
CFRPRC-C60-1-30	30	75	-	12.23
CFRPRC-C60-1-40	40	86	2.12	-

The load –central displacement of slab with combination of three variables is shown in figure 4-14.

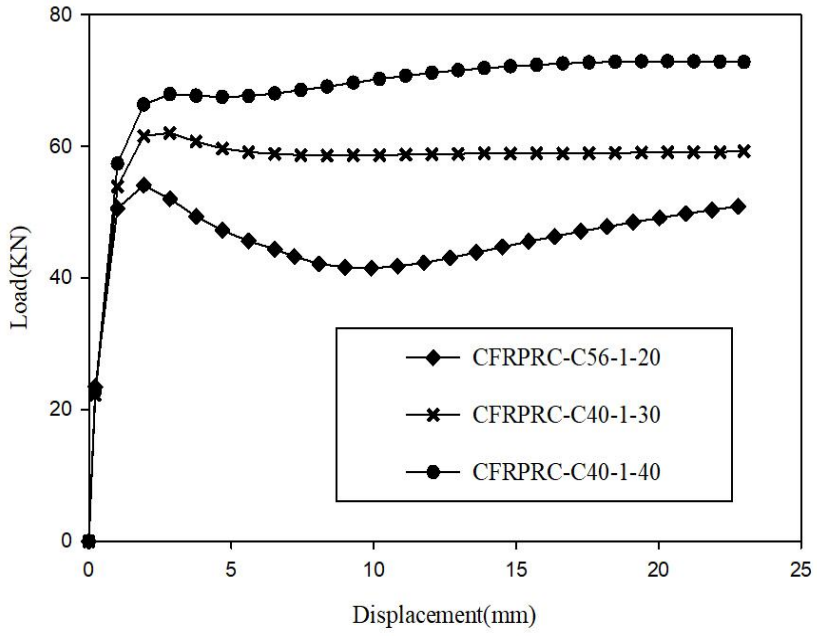

(a) Group 1

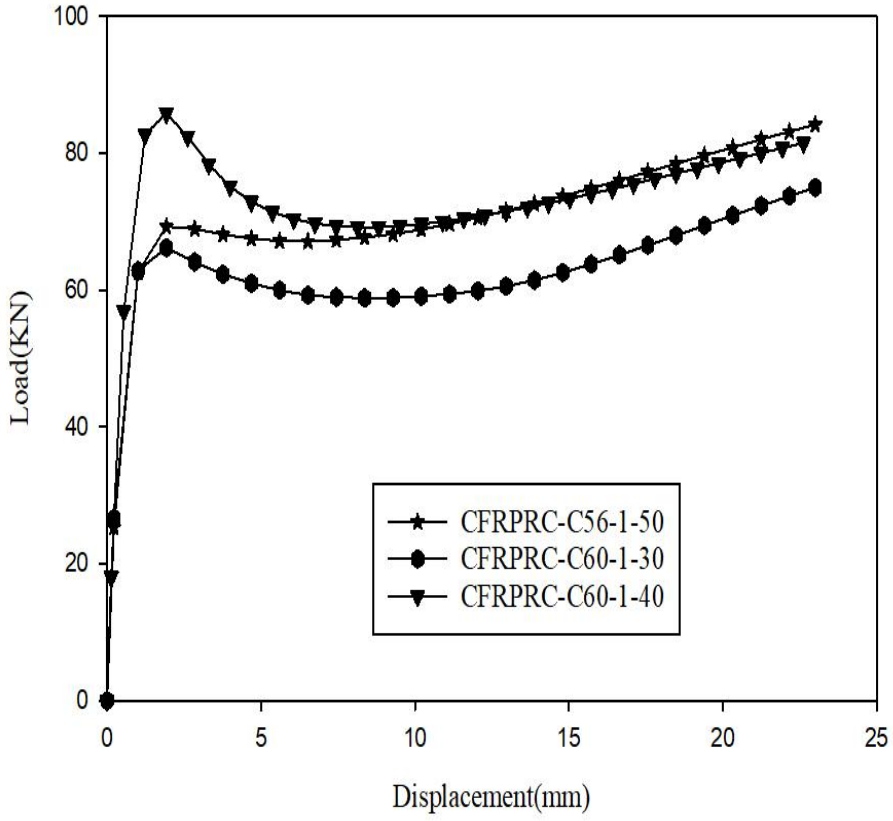

(b) Group 2

Figure 4-14 load –displacement response of slab

Ductility

From table 4.7 the values of ductility ratio of concrete slab specimen CFRPRC-C56-1-50 is lower than CFRPRC-C60-1-30 and CFRPRC-C60-1-40. This shows that low carbon content on CFRP bar with high strength of concrete grade performs well.

Table 4-7 Ductility ratios of CFRP grid reinforced slab (group 2)

Specimens	Δy(mm)	Δu(mm)	$\mu = \frac{\Delta u}{\Delta y}$
CFRPRC-C56-1-50	3.99385	23	5.759
CFRPRC-C60-1-30	1.92385	23	11.955
CFRPRC-C60-1-40	2.15385	23	10.678

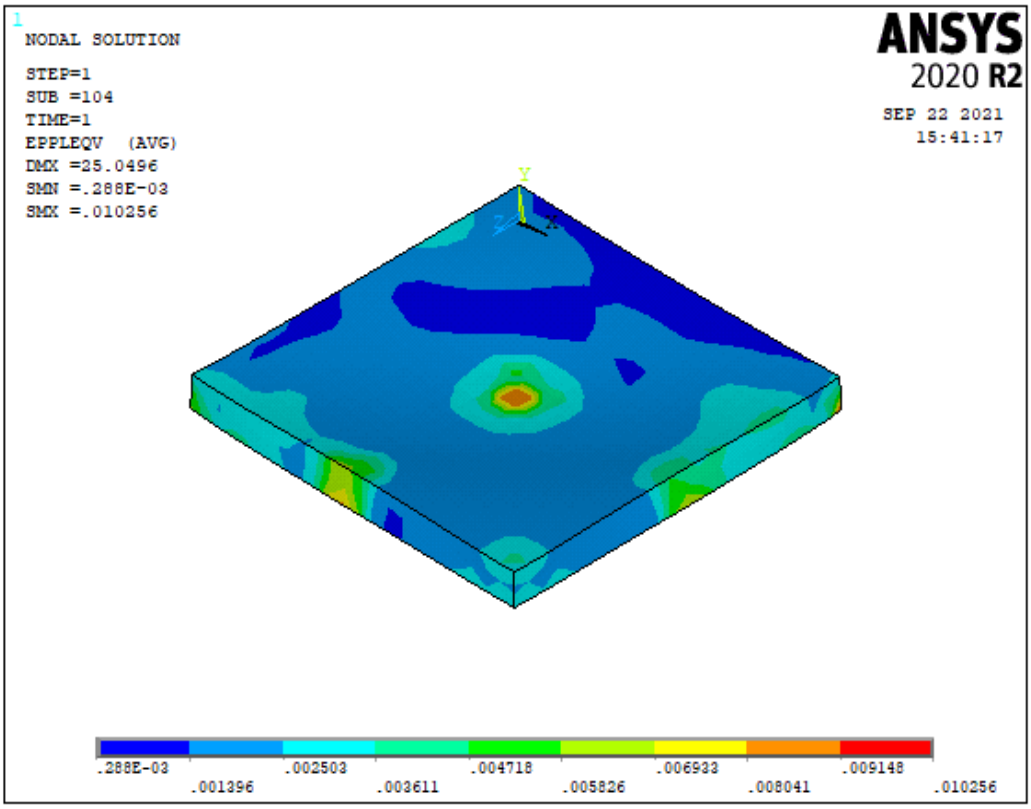

(a) Equivalent plastic strain with CFRPRC-C40-1-30

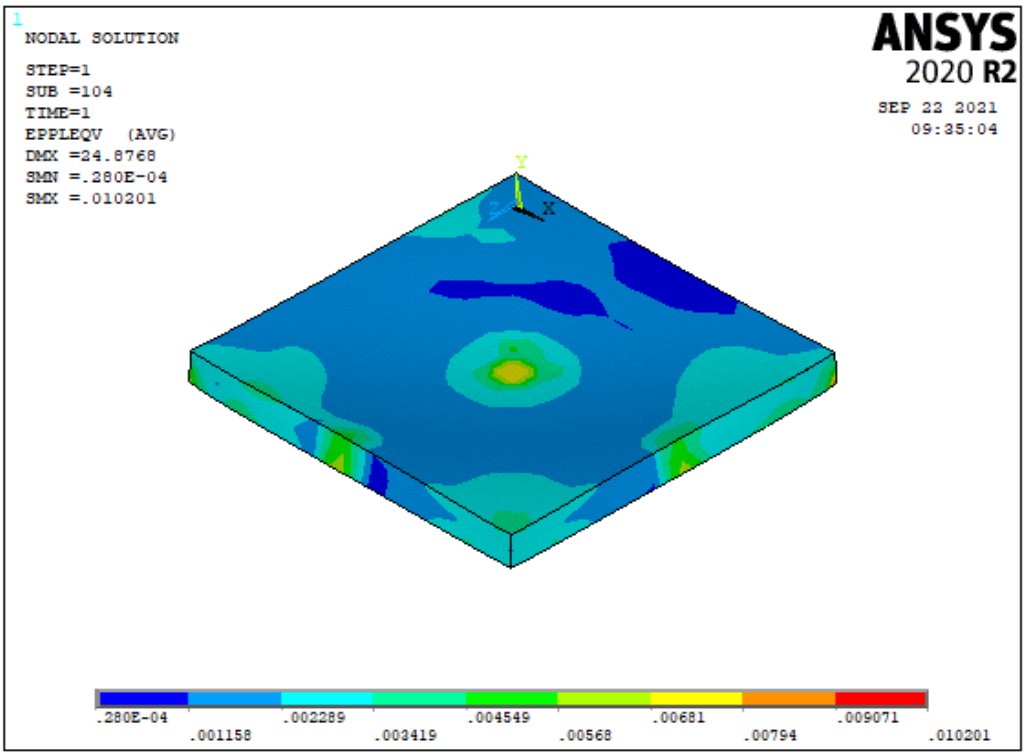

(b) Equivalent plastic strain with CFRPRC-C40-1-40

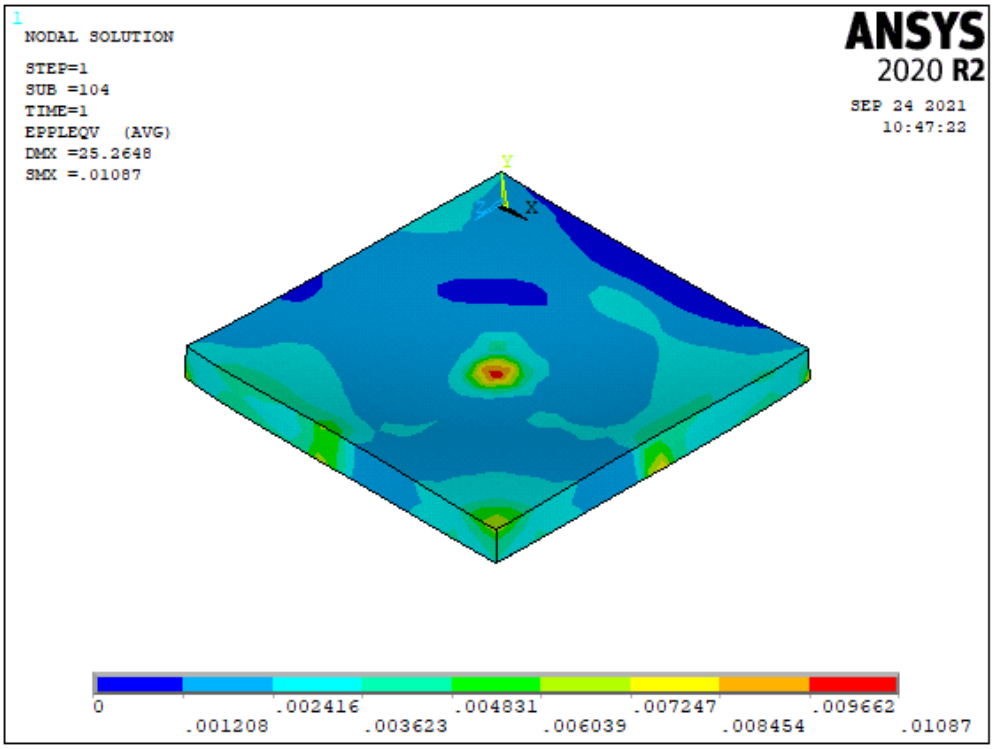

(c) Equivalent plastic strain with CFRPRC-C60-1-30

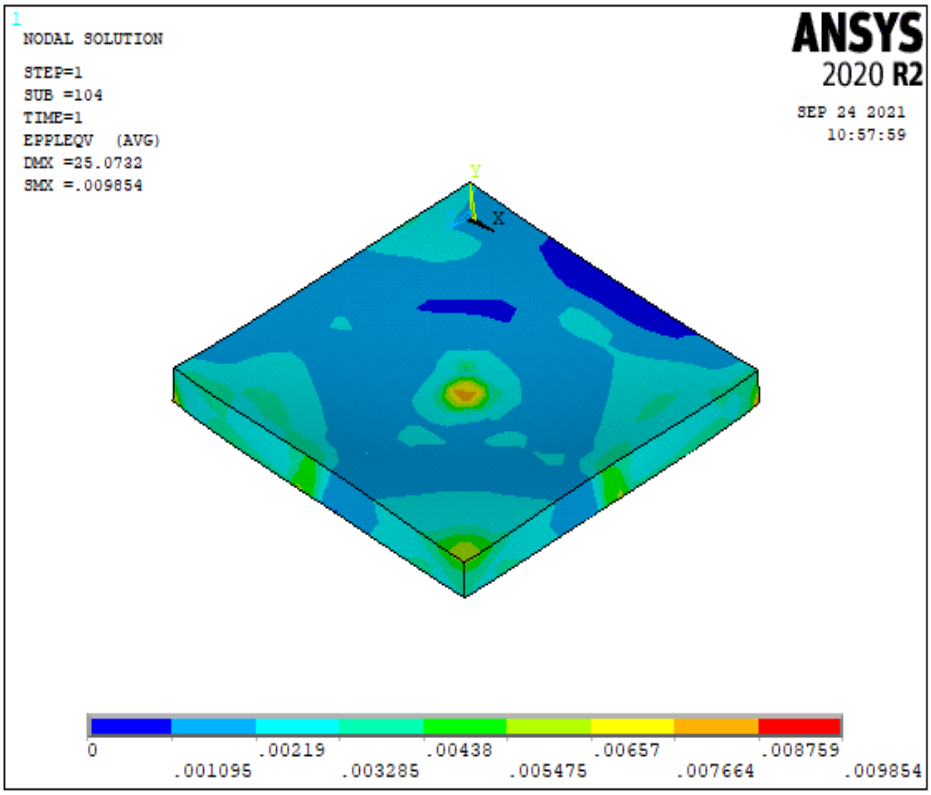

(d)Equivalent plastic strain with CFRPRC-C60-1-40

Figure 4-15 Equivalent plastic strain

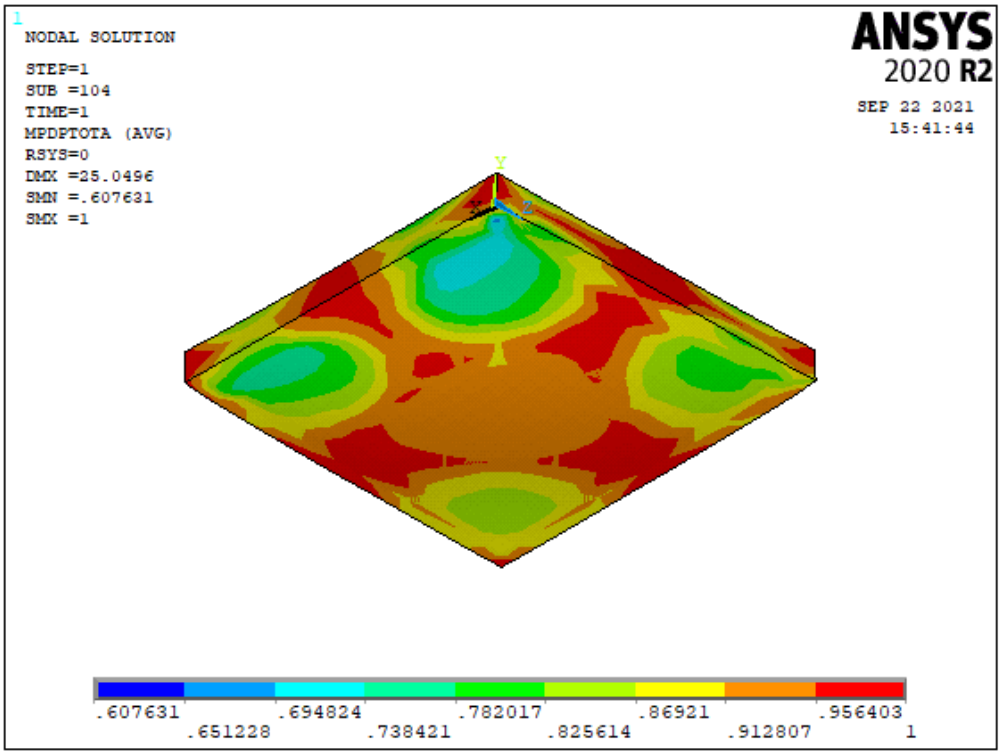

(a) Total damage with CFRPRC-C40-1-30

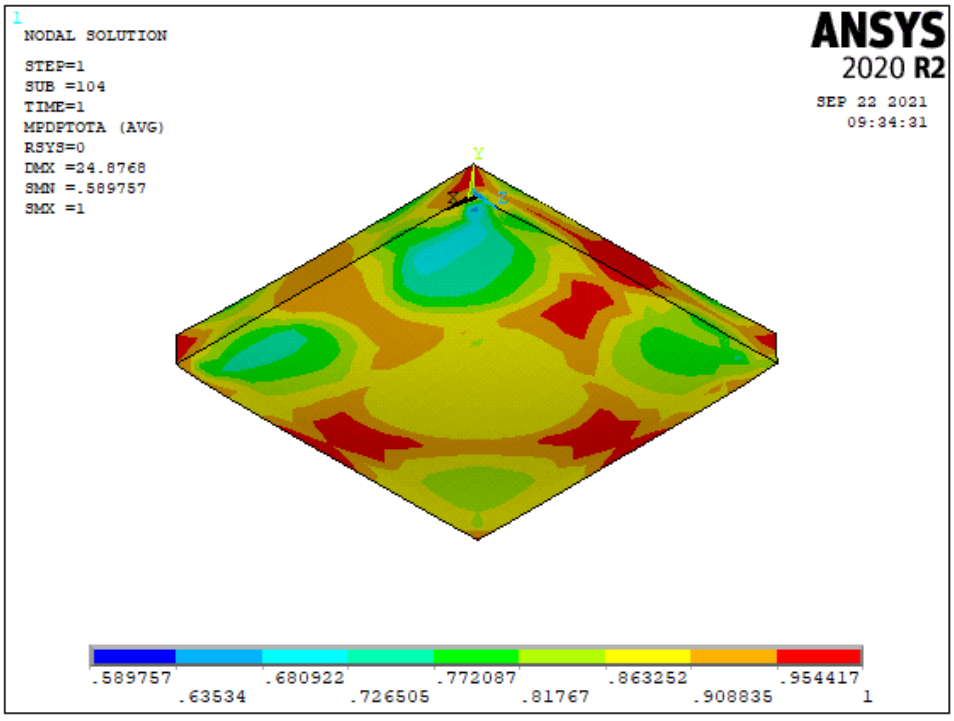

(b) Total damage with CFRPRC-C40-1-40

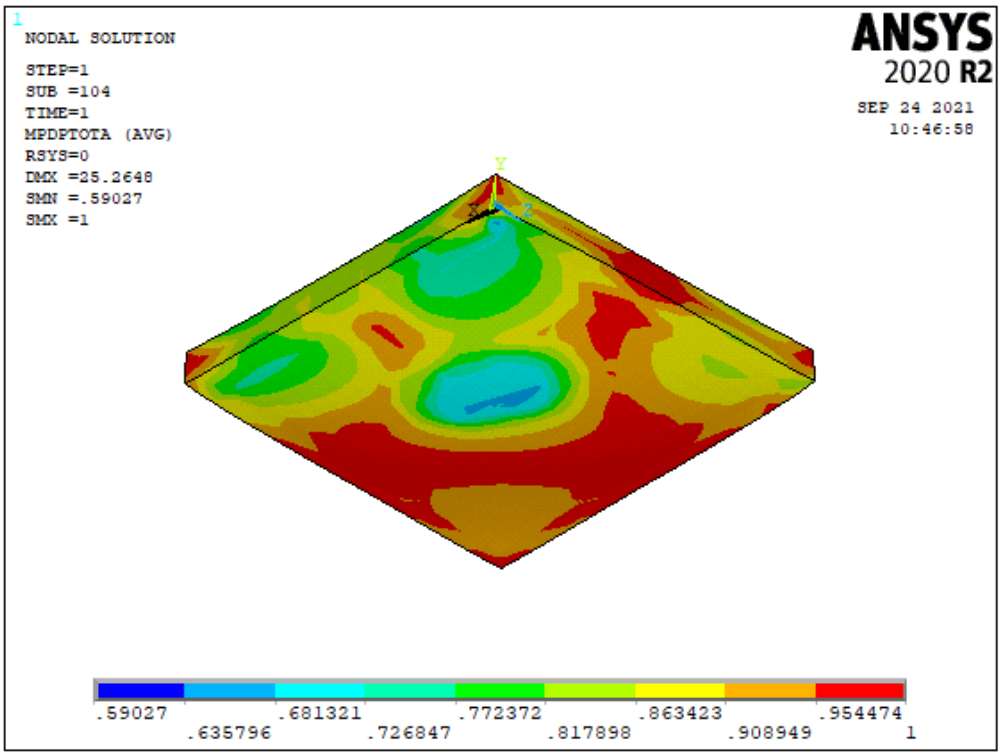

(C) Total damage with CFRPRC-C60-1-30

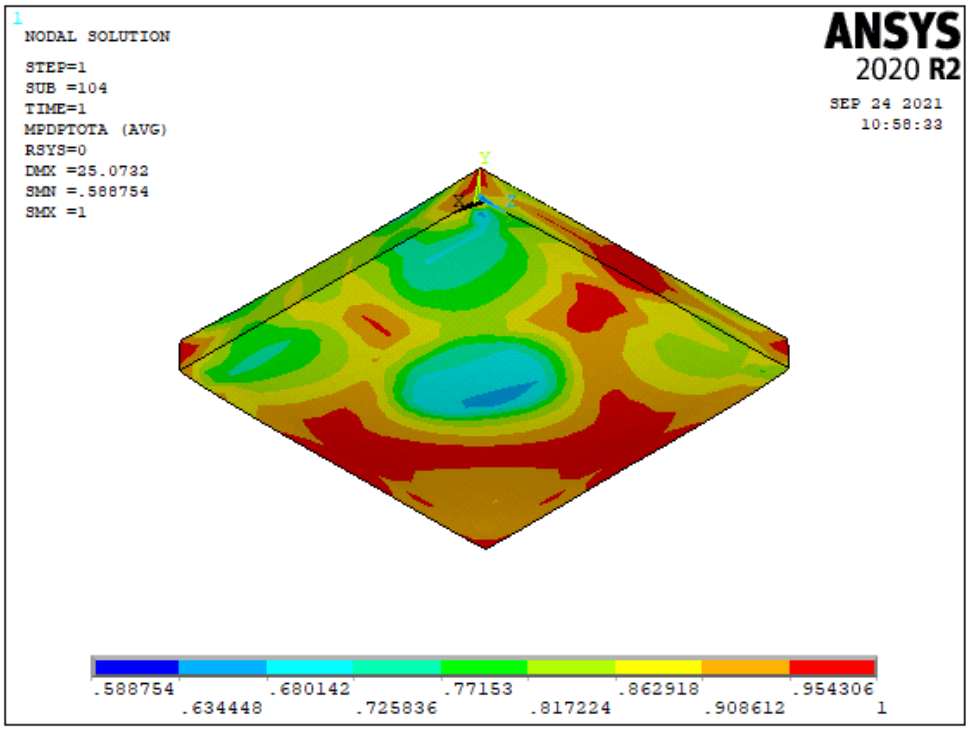

(d) Total damage with CFRPRC-C60-1-40

Figure 4-16 Total damage of concrete in the slab

4.5 Analytical procedure for designing of slab under concentrated load

Comparison in the ultimate load capacity of slab was made for the finite element method and analytical methods. As shown table 4-7 the load capacities of slabs in the two methods shows some difference. The yield line analysis uses rigid plastic theory to evaluate the failure loads corresponding to given plastic moment resistance of the yielded sections were used. It is very economical and versatile method for analysis of two way slabs and estimating the ultimate load carrying capacity, however, this method does not provide any idea about the deflection of the slab at failure and the load at which the first yielding occurs in slab.

ACI code had been presented a yield line analysis method to compute the moments required to resist a concentrated load P if a fan mechanism develops. Assume that the negative-moment capacity is mn and the positive moment capacity is mp per unit width in all directions. Figure 4-17 b shows a triangular segment from the fan in Fig. 4-17a. This segment subtends an angle α and has an outside radius r.

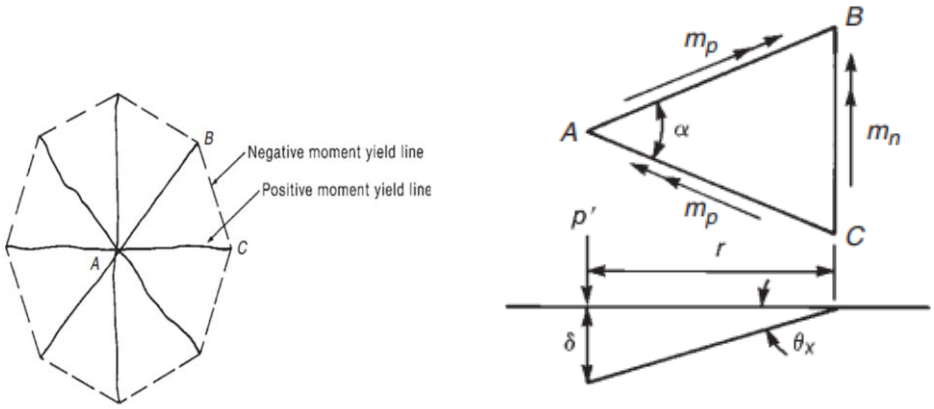

(a) fan yield line around a downward concentrated load at A (b) segment A-B-C

Figure 4-17 Fan yield lines (source: book on reinforced concrete mechanics and design)

Consider the typical triangular slab segment A–B–C in Fig.4-16b: the work done along the positive yield lines can be projected back to the axis of rotation for the slab segment, which is represented by the negative yield line from B–C. Assuming that there are many similar triangular slab segments surrounding the loading point, then the length of line B–C is equal to $\alpha * r$ .As shown in Fig. 14-16b, the rotation of this slab segment, θ_X , is equal to $\frac{\delta}{r}$. Therefore, the internal work done by slab segment A–B–C is

$$\text{IW (A-B-C)} = (mn + mp)\alpha * r * \frac{\delta}{r} = (mn + mp)\alpha * \delta \qquad 4.1$$

The total number of triangular slab segments surrounding the loading point is $\frac{2\pi}{\alpha}$ so, the total internal work is

$$\sum IW = 2\pi(mn + mp) * \delta \qquad 4.2$$

Set internal work equal to external work.

$$\sum IW = 2\pi(mn + mp) * \delta = \sum EW = P * \delta \qquad 4.3$$

$$\Rightarrow mn + mp = \frac{P}{2\pi} \qquad 4.4$$

The nominal flexural strength at a section of can be computed as follows.

$$Mn = As * f_{fu}\left(d - \frac{\beta 1 c}{2}\right) \qquad 4.5$$

Where $\beta 1 = 0.85 - 0.05\frac{f'c - 27.6}{6.7}$ 4.6

C =is the depth to neutral axis and can be calculated as follows.

$$C = \left(\frac{\varepsilon_{cu}}{\varepsilon_{cu} + \varepsilon_{fu}}\right)d \qquad 4.7$$

In this study the area of reinforcement is As =315mm^2, ultimate tensile strength is f_{fu} =496MPa and the effective depth of section is 80mm.

Now substitute equation 4.6 and 4.7 into equation (4.5), we have get,

$$M_n = 9.962\text{KNm/m}$$

Then after the calculation of moment capacity of a slab, the load capacity of slab can be calculated by equating the nominal moment capacity to design moment capacity. Such that,

$$Mn = mn + mp = \frac{P}{2\pi} \qquad 4.8$$

$$\Rightarrow P = 58.56136KN$$

Table 4-8 Comparison of load capacities of slabs using FEM and analytical method

Ultimate load capacity (KN)			
Slab name	Analytical	FEM	% difference
CFRPRC-C56-1-20	58.56136	54.1841	8.15

5. CONCLUSIONS AND RECOMMENDATIONS

5.1 Introduction

This study is aimed to explore the behavior of CFRP grid reinforced two way slabs with a consideration of various parameters under flexural loads. To conduct the study, nonlinear FE analysis was conducted using ANSYS, Mechanical APDL software program. The proposed FE model was validated with the experimental study taken from the literature. The FE model was able to predict the behavior of CFRPRC slab. After validating the model, parametric studies were conducted to study the effect of concrete compressive strength, the effect of bottom CFRP grid reinforcement layer and the effect of volume fraction of carbon fiber on carbon fiber reinforced polymer reinforcement.

5.2 Conclusions

Based on the FE analysis conducted throughout this thesis work, the following conclusions were drawn;

- Slabs with high compressive strength of concrete (60MPa) have better ultimate load resistance than slabs with 40MPa, and 56MPa slabs. It increases

the ultimate load capacity by 15% and 6.9% than slab with 40MPa and 56MPa respectively.

- When the layer of bottom CFRP grid reinforcement is doubled the ultimate load was increased by 29.4% compared with single layer reinforced slabs.
- Increasing the volume fraction of carbon fiber in carbon fiber reinforced polymer reinforcement for slabs was increased the ultimate load of slabs by 6.25% ,19.71% and 35.63% respectively with fiber volume of 30%, 40% and 50% from control specimen with carbon fiber 20%. This is due to the fact that reinforcing fiber in CFRP provides the strength and stiffness to the composite and generally carries most of the applied loads.
- The ultimate load capacity of CFRPRC-C60-1-30 is reduced by 12.23% than CFRPRC-C56-1-50 whereas the ultimate load capacity of CFRPRC-C60-1-40 is almost similar with CFRPRC-C56-1-50 with minimum error 2.12%. In this regard volume fraction of carbon fiber has significant effect than concrete in the ultimate load capacity of CFRPRC slab.

5.3 Recommendations and future works

In this study CFRP grid reinforced two-way slab flexural behavior was conducted. And the following points are forwarded as recommendations.

- CFRP grid can be used effectively as an internal reinforcement in two-way slab systems to address the steel reinforcement corrosion problems.
- The volume fraction of carbon fiber on carbon fiber reinforced polymer reinforced concrete structures has a great effect on the ultimate load resistance than concrete compressive strength.
- Further research needs to be conducted to determine the effect of long term deflection on the structural performance of the slabs reinforced with CFRP grid.

REFERENCES

ACI440R-96,A.C. (2002). *State of the art report on fiber reinforced plastic reinforced for concrete structures.*

ACI440R-96,A.C. (2002). *State of the art report on fiber reinforced plastic reinforced for concrete structures.*

Aljazaeri Z.,Hayder H.Alghazali,and John J.Myers. (2020, March). Effectiveness of using carbon fiber grid systems in reinforced two way concrete slab system. *ACI Structural journal, 117*(2).

Al-Sunna,R.,Pilakoutas,K.,Hajirasouliha,I.,and Guadagnini,M. (2012). Deflection behaviour of FRP reinforced concrete beams and slabs. *Composites*(part B), 2125-2134.

C. Dulude, E. Ahmed, S. El-Gamal & B. Benmokrane. (2010). Testing of Large-Scale Two-Way Concrete Slabs Reinforced with GFRP Bars. *The 5th International Conference on FRP Composites in Civil Engineering.* Beijing,China.

Hatem M. Seliem, Lining Ding, William Potter, and Sami Rizkalla. (2016, September-October). Use of a carbon-fiberreinforced polymer grid for precast concrete piles. *PCI*.

Hesham A. Haggag and Mostafa M. Abd Elsalam. (2020). Flexural Behavior of Two-Way Solid Slabs Reinforced with GFRP Bars. *International Journal of Civil Engineering and Technology, 11*(1), 288-303.

K.J.Bathe. (1996). *Finite element procedures.* New Jersey.

L. Ombres, T. Alkhrdaji, and A. Nanni. (2000). Flexural analysis of one way concrete slabs reinforced with GFRP rebars. *International Meeting on Composite Materials, PLAST 2000, Proceedings, Advancing with Composites*, (pp. 243-250). Crivelli-Visconti, Milan, Italy.

L.C.Hollaway. (2003). The evolution of and the way forward for advanced polymer composites in the civil infrastructure. *Construct.Build.Mater.,17:365*.

Matthys,S. and Taerwe,L. (2000). Concrete Slabs Reinforced with FRP Grids. *Journal of Composites for Construction, 4*(3), 154-161.

N. Banthia,M. AI-Asaly, and S. Ma. (2000, November). Behavior of concrete slabs reinforced with fiber reinforced plastic grid. *journal of Malerials in Civil Engineering, 7*(4), 252-257.

Piyush K. Dutta, David M. Bailey, Stephen W. Tsai, and David W. Jensen. (1998). *Composite Grids for Reinforcement of Concrete Structures.*

Q. Z. Khan, M. Ali, A. Ahmad, A. Raza , and M. Iqbal. (2021, January 11). Experimental and fnite element analysis of hybrid fber reinforced concrete two-way slabs at ultimate limit state. *SN Applied Sciences*.

R. Sivagamasundari and G. Kumaran. (2008). Effect of Glass Fibre Reinforced Polymer Reinforcements on the Flexural Strength of Concrete One Way Slabs under Static and Repeated Loadings. *Asian Journal of Applied Sciences I, 1*, 19-32.

Rahman,A.H.,Kingsley,C.Y.,Kobayashi,K. (2000, February). Service and ultimate load behavior of bridge deck reinforced with carbon FRP grid. *Journal of Composites for Construction, 4*.

Rizkalla, S., and Tadros, G. (1994). First smart bridge in Canada. *ACI Concrete Int., 16(6),* 42–44.

S. El-Gamal, E. El-Salakawy, and B. Benmokrane. (2007). Influence of Reinforcement on the Behavior of Concrete Bridge Deck Slabs Reinforced with FRP Bars. *Journal of Composites for Construction, 11*(5), 449-458.

S.T. Smith & R.I. Gilbert. (2003). Tests on RC slabs reinforced with 500 MPa welded wire fabric. *Australian Journal of Civil Engineering, 1*(1), 59-66.

Saim R, Muhammad K. I. Khan , Scott J. Menegon , Hing-Ho Tsang, and John L. Wilson. (2019). Strengthening and Repair of Reinforced Concrete Columns by Jacketing: State-of-the-Art Review. *Sustainability*.

T.Uomoto, H.Mutsuyoshi, F.Katsuki, and S. Misra. (2002, June 1). Use of Fiber Reinforced Polymer Composites as Reinforcing Material for Concrete. *Journal of Materials in Civil Engineering, 14*(3), 191-209.

Taerue, L. (1993). FRP Developments and Applications in Europe," Fiber-Reinforced Plastic (FRP) Reinforcement for Concrete Structures: Properties and Applications. 99-113.

Thomas H.Courtney, T. (1990). Mechanical behavior of materials. *McGraw,Hill*.

W.Meng and K.H.Khayat. (2016). Experimental and Numerical Studies on Flexural Behavior of Ultra-High Performance Concrete Panels Reinforced with Embedded Glass Fiber-Reinforced Polymer Grids. *Journal of the Transportation Research Board*, 38-44.

Yost, J. R. (1993). *Fiber-reinforced plastic grids for the structural reinforcement of concrete beams.* Doctoral Dissertations.1770.

Yost,J.R.,and Schmeckpepers,E.R. (2001, December). Strength and serviceability of FRP grid reinforced bridge decks . *Journal of Bridge Engineering, 6*, 605-612.

Z. Sakka and R. Ian Gilbert. (2017). *Numerical Investigation on the Structural Behavior of Two-way Slabs.* The 2017 Congress on Advances in structural engineering and mechanics (ASEM17), llsan(seoul),korea.

Zreid, I. & Kaliske, M. (2018). A gradient enhanced plasticity-damage microplane model for concrete. *Computational Mechanics*.

APPENDIX

Appendix-A: Thesis ANSYS Mechanical APDL Code

This chapter presents the ANSYS mechanical APDL code used for this thesis work. APDL code is for typical specimen, S-1

Material property

E = 33960

nu = .2

fuc = 56

fbc = 1.15*fuc

fut = 0

Rt = 1

Dx = 45500

sigVc0 = -30

R = 2

c = 100000

m = 2.5

gamt0 = 0

gamc0 = 2e-5

betat = 8000

betac = 5000

MP, EX, 1, E

MP, NUXY, 1, nu

```
TBDATA, 1, fuc, fbc, fut, Rt, Dx, sigVc0
TBDATA, 7, R, gamt0, gamc0, betat, betac
TB, MPLA, 1,,, NLOCAL
TBDATA, 1, c, m
MP, EX, 2, 200000
MP,EX, 2, 0.3
MP, EX, 3, 55850
MP, NUXY, 3, 0.3
MP, EX, 4, 67570
MP, NUXY, 4, 0.3
```

```
Concrete geometry and mesh
/prep7
e1= 50mm! Element size e1 in mm
! Create concrete block
block, 0, 1150, 0, 100, 0, 1150
! Create loading plate
block, 500,650,100,150,500,650
 ! Compress area and volume numbers
ALLSEL, ALL
NUMCMP, LINE
```

```
NUMCMP, AREA

NUMCMP, VOLUME

! Mesh areas

LSEL, All

Lesize, all, e1

! Hex. Meshing (brick element meshing)

! Mesh concrete

TYPE,   100

MAT,     1

REAL,

ESYS,   0

SECNUM, ,

ALLSEL, ALL

MSHKEY, 1          !1=mapped meshing

MSHAPE, 0, 3d        ! Hexagonal element

CHKMSH,'VOLU'

VMESH, ALL

! Change loading plate material number

ALLSEL, ALL

VSEL, ALL

VSEL, S,, , 2,

ESLV, R

MPCHG, 2, ALL,
```

```
!merges all similar nodes and elements

esel, all

NSEL, ALL

NUMMRG, NODE,,,, LOW

NUMMRG, KP,,,, LOW

CFRP reinforcement

/prep7

NUMCMP, LINE     ! Compress line number

NUMCMP, AREA     ! Compress area

! Define discrete reinforcing sections

SECTYPE, 1, REINF, DISC      ! Section reference#1

SECDATA, 3, 7.2, mesh        ! Section data; material 3, rebar x-
sectional area 7.2mm2

SECTYPE, 2, REINF, DISC      ! Section reference#2

SECDATA, 4, 9.0, mesh       ! Section data; material 4, rebar x-
sectional area 9.0mm2

!!!!!!!!!!!!!!!!!!!!!!!!!!!!!!!!!!!!!!!!!!!!!!!!!!!!!!!!!!!!!!!!!!!!!!!!!!!!!!!!!!!!!!!!!!!
!!!!!!!!!!!!!!!!!!!!!!!

! Bottom bar

! Transverse rebar

! creat one line element and copy paste into 34 location to get

! 35 main rebars parallel to Z- axis
```

```
 ! Concrete cover 20mm
k,1000,25,20,25     ! Create key point 1000
k,1001,25,20,1125   ! Create key point 1001
l,1000,1001         ! Create line using above key points to generate Eighteen
main rebar parallel to Z-axis
*GET, nn1, LINE, 0, NUM, MAX, ,          ! Assign nn1 = above created
line number
LSEL,S, , , nn1                          ! Selected line number nn1
LGEN,1+34,all, , ,30, , , ,0             ! Copy paste line number nn1 to
generate additional 34 bars at 30mm spacing in X-direction
! Mesh rebars
ET, 200, 200,2 ! Mesh200 place holder
! Mesh
TYPE,   200
MAT,       3
REAL,
ESYS,      0
SECNUM, 1
LSEL, S, , , nn1
Lesize,all,,,1
LSEL,S, , , nn1
lmesh,all
esel,all
nsel,all
EREINF
! Longitudinal Main rebars
! Create one line element and copy paste into 34 locations to get
! 35 main rebars parallel to X- axis
! Concrete cover 20mm
k,1002,25,20,25       ! creat key point 1002
k,1003,1125,20,25     ! creat key point 1003
```

```
l,1002,1003          ! Create line using above key points to generate one
main rebar parallel to X-axis
*GET, nn2, LINE, 0, NUM, MAX, ,    ! Assign nn2 = above created line
number
LSEL,S, , , nn2                   ! Selected line number nn2
LGEN,1+34,all, , , , ,30, ,0       ! Copy paste line number nn2 to generate
additional 34 bars at 30mm spacing in Z-direction
!!!!!!!!!!!!!!!!!!!!!!!!!!!!!!!!!!!!!!!!!!!!!!!!!!!!!!!!!!!!!!!!!!!!!!!!!!!!!!!!!!!!!!!!!!!!
!!!!!!!!!!!!!!!!!!
! Mesh main rebar
ET, 200, 200,2 ! Mesh200 place holder
! Mesh
TYPE,   200
MAT,       4
REAL,
SECNUM, 2
LSEL, S, , , nn2
Lesize, all,,,1
LSEL,S, , , nn2
lmesh,all
esel,all
nsel,all
EREINF
! Top bar
! Transverse rebar
! Create one line element and copy paste into 34 locations to get
! 35 main rebars parallel to Z- axis
! Concrete cover 20mm
k,1004,25,87.5,25     ! Create key point 1004
k,1005,25,87.5,1125   ! Create key point 1005
l,1004,1005         ! Create line using above key points to generate fifteen
main rebar parallel to Z-axis
```

```
*GET, nn3, LINE, 0, NUM, MAX, ,          ! Assign nn3 = above created line number
LSEL,S, , , nn3                          ! Selected line number nn3
LGEN,1+34,all, , ,30 , , , ,0            ! Copy paste line number nn3 to generate additional 34bars at 30mm spacing in X-direction

! Mesh rebars
ET, 200, 200,2 ! Mesh200 place holder
! Mesh
TYPE,   200
MAT,       3
REAL,
ESYS,      0
SECNUM, 1
LSEL,S, , , nn3
Lesize,all,,,1
LSEL,S, , , nn3
lmesh,all
esel,all
nsel,all
EREINF
! Longitudinal Main rebar
! Create one line element and copy paste into 34 locations to get
! 35 main rebars parallel to X- axis
! Concrete cover 20mm
k,1006,25,87.5,25       ! Create key point 1006
k,1007,1125,87.5,25     ! Create key point 1007
l,1006,1007             ! Create line using above key points to generate one main rebar parallel to X-axis
```

```
*GET, nn4, LINE, 0, NUM, MAX, ,     ! Assign nn4 = above created
line number
LSEL,S, , , nn4                    ! Selected line number nn4
LGEN,1+34,all, , , , ,30 , ,0       ! Copy paste line number nn4 to
generate additional 34 bars at 30mm spacing in Z-direction
!!!!!!!!!!!!!!!!!!!!!!!!!!!!!!!!!!!!!!!!!!!!!!!!!!!!!!!!!!!!!!!!!!!!!!!!!!!!!!!!!!!!!!!!
!!!!!!!!!!!!!!!!!!!!
! Mesh main rebar
ET,200,200,2 ! Mesh200 place holder
! Mesh
TYPE,   200
MAT,       4
REAL,
ESYS,       0
SECNUM, 2
LSEL,S, , , nn4
Lesize,all,,,1
LSEL,S, , , nn4
lmesh,all
esel,all
nsel,all
EREINF
NUMMRG, NODE, , , ,LOW
NUMMRG, KP, , , ,LOW
Micro plane text
ALLSEL, ALL
ESEL, ALL
ESEL, S, TYPE,, 100
EMODIF, ALL, TYPE, 1,
! Delete Element 185
ETDEL, 100
```

```
 Loading and boundary conditions
Solution
/SOL
! Boundary condition
NSEL, S, LOC, Y, 0
NSEL, R, LOC, X, 50, 1100
NSEL, R, LOC, Z, 50
D, ALL, UY, 0
D, ALL, UX, 0
D, ALL, UZ, 0
NSEL, S, LOC, Y, 0
NSEL, R, LOC, X, 50, 1100
NSEL, R, LOC, Z, 1100
D, AL, UY, 0
NSEL, S, LOC, Y, 0
NSEL, R, LOC, Z, 50, 1100
NSEL, R, LOC, X, 50
D, ALL, UY, 0
NSEL,S, LOC,Y,0
NSEL,R, LOC,Z,50,1100
NSEL,R ,LOC,X,1100
D, ALL, UY, 0
! Loading
NSEL, S, LOC, Y,150                ! 32 total number of node on plate
D, ALL, UY,-23
esel,all
nsel,all
TIME,1
NSUBST, 600,800,100, on       ! Load Sub steps
OUTRES, ALL,1              ! WRITE ALL OUTPUT
SOLVE
SAVE
FINISH
```

```
! Concrete damage plots
/POST1
esel, s,Mat,,1    ! Select concrete material
/trlcy, elem, 0
SET, LAST
plnsol, eppl, eqv          ! Plot major cracks, equivalent plastic strain
/POST1
esel, s,Mat,,1
/trlcy, elem, 0
SET, LAST
plnsol, MPDP,TOTA ! Plot minor cracks
/POST1
esel, s,type,,201
plnsol, eppl, eqv  ! Plot rebars equivalent plastic strain
/wait, 1
Result for load displacement curve
Finish
/prep7
 ! Loading nodes
 NSEL, R, LOC, Y,150
*GET, n_min, NODE, 0, NUM, MIN, ,
*GET, n_max, NODE, 0, NUM, MAX, ,
*GET, n_count, NODE, 0, COUNT, , ,
Finish
/POST1
SET,LAST
finish
/POST26
ii=n_min
```

```
*do,i,1,n_count-1,1
rforce,2, ii,F,y,FY
ADD, 3, 3, 2,,FYT,,,,-0.001,     !0.001 is to change force N into KN out
put
ii=NDNEXT(ii)
*ENDDO
n_uy=NODE (575, 0,575)   ! node coordinate at which deflection is read,
here Uy deflection or set n_uy = node number
NSOL,4,n_uy,U,Y,UY
ABS,4,4,,,UY
/AXlab,X,displacement [mm]
/AXlab,Y,force [kN]
XVAR, 4
PLVAR, 3
```